THE DECONTAMINATION OF RADIOACTIVE ION EXCHANGE RESINS USING NEUTRAL SALTS AS ELUTRIANTS

Joseph S. Baron

Edward A. Mason

N. Thomas Olson

MITNE-133

Nuclear Engineering Department

Massachusetts Institute of Technology

July 1971

THE DECONTAMINATION OF RADIOACTIVE ION EXCHANGE RESINS USING NEUTRAL SALTS AS ELUTRIANTS

Joseph S. Baron

Edward A. Mason

N. Thomas Olson

MITNE-133

Nuclear Engineering Department

Massachusetts Institute of Technology

July 1971

ABSTRACT

An effective means of concentrating the radioactivity found on demineralizers in a water-cooled nuclear reactor's primary coolant system was sought. Elution experiments using sodium and ferric chloride/sulfate salts as eluting agents were conducted. The most tightly bound ions from valence groups -1 to +4 were used to represent their valence groups. Operational parameters investigated included flow rate, temperature, and eluant concentration.

Experiments showed that for the heavy, polyvalent, metal ions, the sulfate anion proved extremely effective in aiding the elution through complexing. Elevated temperatures which increased the diffusional rate, decreased the complexing. The result is that increased temperatures are of no advantage. Extremely low flow rates (~.01gpm/ft^2) would have to be used to compensate for the polyvalent ion's low diffusional rate in the resin. Concentrated ferric sulfate solutions (~ 1N) were found to be effective in concentrating the radioactivity.

For ions in valence groups +1 and +2, dilute ferric chloride solutions (~ 1/7N) at ambient temperatures were used to take advantage of the iron's higher valence (mass action law) and to avoid precipitation of the alkaline earths by the sulfate anion. Ferric salts could not be used for elution of the anionic resins due to a redox reaction with iodide which deposited iodine in the resin. Sodium sulfate was used with better results.

The radioactivity can be concentrated in the range of 4 to 40 times depending on the particular ions involved and their mixture.

TABLE OF CONTENTS

LIST OF FIGURES

LIST OF TABLES

CHAPTER I

INTRODUCTION

In water-cooled nuclear reactors, fission products, activated corrosion products, and impurities in the makeup water constitute the radioactive burden of the primary coolant loop. It is desirable to reduce this contamination to a low level in order to prevent fouling of heat transfer surfaces, to facilitate maintenance, and to minimize the effect of any leakage.

Since the concentrations of the contaminants in the coolant are low, substantial removal or concentration is difficult. In nuclear plants like Connecticut Yankee, cobalt-58 (1) has been a particular problem. It is formed in an (n, p) reaction on nickel-58-bearing alloys and deposited as crud throughout the coolant system. When the reactor was shutdown and depressurized for refueling in April, 1969 (the purification system did not operate in this condition), the crud resolubilized and the activity in the primary coolant rose to 0.4 Ci/ml., corresponding to a concentration of $1.28 \cdot 10^{-5}$ g/ml. Once repressurized, this contamination loaded the exchanger to a high level of activity.

Synthetic ion exchange resins such as Dowex HCR-W, a strong acid cation exchanger, and Dowex SBR-P, a strong

base anion exchanger, are used in mixed form for purification of nuclear reactor water coolant streams. These mixed ion exchangers are very rarely utilized to full capacity; the determining factor being the radiation level outside the exchange column. In present day practice these resins are not regenerated but are shipped off-site for disposal. Connecticut Yankee is an exception to this rule. Their resin has been stored on-site since it is too radioactive for their resin shipping casks.

The prohibitively high cost of regeneration, the reduced capacity due to radiation damage, and the desire of the electric utility companies to minimize on-site chemical processing of radioactive material tend to maintain this practice. However the overall cost of disposal is high and has essentially two components (2). First is the cost of transporting the radioactive ion exchange resin plus its shielding and second is the cost of the final disposition of the radioactive waste.

Of the two costs, it is in the cost of transportation that the utilities could most readily effect cost reductions. As the major fraction of the cost is for shipping the shielding, a means of reducing the shielding weight could realize a savings.

One possible means of decreasing the shielding is to elute the radioactive ions from the resin. Evaporation of

the solvent and shipment of the dried, solid radioactive residue could be effective in reducing costs if the volume of residue requiring shielding during shipment was substantially below that of the ion exchange resin. The resin would be essentially decontaminated and would thus require very little shielding during shipment for disposal.

Under the criterion that the volume of dry residue be substantially smaller than the volume of the exchanger, the use as eluting agents of strong acids/bases or neutral salts was investigated. Strong acids/bases were found to be ineffective for the elution while the patent of John H. Noble at Stone and Webster Engineering Co. (37) indicated that neutral salts could effect a major reduction in residue volume.

The strong acids/bases case was evaluated using the data of Nelson, Maurase, and Kraus (17, 18, 19). Their work provided experimental data on the effect of acid concentration on elemental ion exchange distribution coefficients. This information combined with the chromatographic elution Equation (4)

$$v_{max} = X(D + \delta) \qquad (1)$$

v_{max} is the volume of eluting solution necessary for the appearance of the concentration maximum of the band in the effluent after passage through the column,

X is the volume of the column,

D is the volumetric distribution coefficient,

δ is the void fraction of the column (usually $\sim .4$),

indicated that strong acids would not fulfill the requirement of small residue volume relative to that of the resin.

A sample calculation will illustrate this. Barium will be used since it is representative of ions that are tightly bound to the exchanger. Using HCl as the elutriant, the concentration at which the barium distribution coefficient is a minimum was chosen ($D_{min} = 9$ at 6M HCl). Under these conditions and a resin volume of 1000 cc (Dowex 50x4; capacity: 5.12 equivalents per kg dry hydrogen form resin; density: .29 kg/l in water), the volume of elutriant required for the complete elution of barium is 9.41 (56.4 gm-moles of HCl). Neutralization of the HCl with NaOH and evaporation of the solvent leaves a salt residue with a volume of 1520 cc.

$$\frac{(56.4)(M\ W_{NaCl})}{(\rho_{NaCl})} = \text{Volume of Residue} \qquad (2)$$

$$\frac{(56.4)(58.5)}{2.16} = 1520 \text{ cc}$$

$M W_{NaCl}$ is the salt's gm molecular weight, 58.5 gm/gm mole

ρ_{NaCl} is the salt's crystal density, 2.16 gm/cc

This volume is 1.5 times the volume of resin, and hence would not reduce the shielding at all. Therefore if the volume of dried eluting agent is to be less than that of the ion exchanger, HCl and strong acids in general are excluded as possible eluting agents. For strong base quarternary ammonium anion resins, the selectivity coefficients of the halogens relative to the hydroxyl ion are greater than one (4); therefore halogen-halogen distribution coefficients (6) provide the necessary information for the same type calculation (D_{min} (bromide to chloride) = 9 at 6.5 M LiCl). Using Equation (1), the complete elution of bromide would require 9.4 l (61.1 gm-mole LiCl) for 1000 cc of anion resin (Dowex-1). Substituting the appropriate values for LiCl in Equation (2) (ρ_{LiCl} = 2.07 gm/cc; $M W_{LiCl}$ = 42.4), yields a dry residue volume of 1250 cc again a value greater than the resin volume. If the hydroxyl ion had been used, this value for the volume would have been even larger, thus eliminating strong bases as eluting agents.

The use of neutral salts offered the possibility of reducing the amount of elutriant needed. Since the treated exchanger is not required to be in its original form but

only to be free from radioactivity, eluting ions with a high affinity for the resin phase would be preferred as eluting agents in order to keep the amount of elutriant to a minimum. These neutral salts should be used in acidic solutions to prevent the precipitation of metal hydroxides.

In terms of conventional elution processes, there are many similarities between elution with hydrogen and with another cation. In an elution process using a neutral salt, the same procedural steps of backwashing, resin separation, and the like occur as if the elutriant were a strong acid or base.

The present study is concerned with only the elution step and how, once the neutral salt has been chosen, the operating conditions of salt concentration, flow rate, and temperature affect the residual salt volume.

CHAPTER II

THEORY OF SELECTIVITY

In the development of any commercial process, experimental data provide a set of points which delimit an operating range for that process. Extrapolation beyond this range requires an understanding of the physical effects related to the process. For the case of ion-exchange, knowledge concerning the factors influencing the equilibrium and, in turn, the selectivity is needed. If these are understood, improvement in the effectiveness of the elution by reducing the amount of elutriant required may be possible.

In the "equilibrium" case of elution, the ion exchanger is in equilibrium with its contacting solution. The elution of a resin under "equilibrium" conditions represents the minimal amount of eluting agent required for the eluant, its concentration, and the temperature. However, operation under equilibrium conditions requires an almost infinite amount of time by having flow rates only a small increment above zero in order to achieve a quasi-equilibrium state at every point in the column. As this is infeasible, operation under "non-equilibrium" conditions is used and necessitates the use of a larger volume of elutriant. However the selectivity is not a constant and depends

upon the eluant concentration and temperature, operating under different eluant conditions could change the amount of elutriant needed.

For operation under different eluant conditions, a quantitative calculation of the change in the amount of eluant necessary for elution could be made in the equilibrium case relative to some eluant condition where the amount of elutriant needed for elution is known. In the non-equilibrium case, this may or may not be possible and only the sign of the elutriant volume change may be predicted.

Thus it is important to establish a physical understanding of the effects influencing the exchange process since they will be useful in evaluating the experimental results. The ensuing presentation provides a physical picture of selectivity and describes the major effects influencing it for ion exchangers such as Dowex HCR-W or Dowex SBR-P in aqueous systems.

In setting up an expression for the exchange equilibrium between ions A and B of charge a and b respectively and of the same polarity, the resin phase is considered to be a concentrated electrolyte solution (3, 6, 7, 8).

$$|a|B^{b} + |b|\overline{A}^{a} \rightleftarrows |a|\overline{B}^{b} + |b|A^{a} \qquad (3)$$

The bar indicates the resin phase. If the same standard

states are chosen for the ions in the resin and the aqueous phases (unit activity coefficients in an infinitely dilute solution), the equilibrium expression is

$$Q_{B/A} = \frac{(\bar{B})^{|a|}(A)^{|b|}}{(B)^{|a|}(\bar{A})^{|b|}} = \frac{[\bar{B}]^{|a|}[A]^{|b|}\,\bar{\gamma}^{|a|}\;\gamma_A^{|b|}}{[B]^{|a|}[\bar{A}]^{|b|}\,\gamma^{|a|}\;\bar{\gamma}^{|b|}} \qquad (4)$$

$$= K_{B/A}\,\Gamma_{B/A}$$

( ) represent activities

[ ] represent concentrations, moles/liter

γ is the ion activity coefficient

$K_{B/A}$ is the selectivity coefficient

$Q_{B/A}$ is the thermodynamic equilibrium constant

Rewriting Equation (4) in terms of equivalent fractions of the exchanging ion, B , results in Equation (5) after a suitable rearrangement of terms.

$$\frac{R_{X_B}{}^{|a|}}{(1-R_{X_B})^{|b|}} = \frac{X_B{}^{|a|}}{(1-X_B)^{|b|}}\,\frac{C_R{}^{|b|-|a|}}{C^{|b|-|a|}}\,Q_{/A}\,\frac{\gamma_B^{|a|}\;\bar{\gamma}_A^{|b|}}{\bar{\gamma}_B^{|a|}\;\gamma_A^{|b|}} \qquad (5)$$

R_{X_B} is the equivalent fraction in the resin,

X_B is the equivalent fraction in solution,

C_R is the capacity of the resin, equivalent/liter resin,

C is the normality of the solution.

Equation (5) represents the relationship between the equivalent fractions of the exchanging ions in each phase in terms of an "apparent" selectivity coefficient. This "apparent" selectivity is composed of the activity coefficients, the equilibrium constant, and the ratio of the ionic concentrations of the two phases to the $|b| - |a|$ power. If the activity coefficients are grouped with the equilibrium constant, the effect of solution concentration (mass action effect) can be shown (20). Since C_R is a fixed value determined by the resin chosen, the selectivity of the resin for the higher valence ion is shown to be inversely proportional to the total equivalent concentration in the solvent to the $|b| - |a|$ power. That is, if is the higher valence ion, B would show an increasing preference for the resin phase as the solution became more dilute. Conversely if the valence of B was the smaller, the preference of B would increase with increasing concentration of exchanging solution demonstrating the mass action effect.

In terms of the elution process, it is desirable to consider using a polyvalent ion as the eluting species in order to reduce the amount of neutral salt needed for the elution. As seen from mass action law, it is desirable to use a dilute solution when the ion to be eluted is of lower valence than the eluting ion and a concentrated solu-

tion of the eluted ion's valence is higher. In the case where the eluting ion's valence is the same as that of the eluted ion, the selectivity of the resin is not concentration dependent and the amount of eluant required is also concentration independent.

The degree of exchange or the selectivity in Equation (4) depends upon the activity coefficients of the exchanging ions. In dilute solutions, the aqueous phase activity-coefficient ratio tends to unity and the degree of exchange depends on the resin phase activity coefficients.

Selectivity could be qualitatively predicted if the activity coefficients of the resin monomer species for A and B in the aqueous phase were known. However the differences between an aqueous electrolyte solution and the resin phase would have to be taken into consideration. The major differences are that one type of ion is fixed on the resin matrix, that the hydrocarbon matrix itself disturbs the water structure inside the resin, and that the elastic properties of the hydrocarbon matrix affect the exchange process. Corrections for these differences are needed if the selectivity is to be predicted.

Various models, as described in Helfferich (5), have attempted to account for the major resin phase interactions. Diamond and Whitney (6, 7, 8) have

developed a qualitative description of the ion exchange selectivity process. They consider the different types of possible interactions and estimate which effect predominates and how their comparative importance shifts under varying conditions. The important effects are water-water, ion-water, ion-ion, and ion-resin matrix interactions.

Water-Water

At room temperature, water molecules form a highly-hydrogen-bonded network with strong intermolecular forces. This tendency of water molecules to bond to each other has two important consequences. First, the water structure tends to reject any other species unless the other has hydrophilic groups or is charged. If the water structure is disrupted, it can more readily accept a foreign species. This happens inside the resin since the internal phase water is constricted by the resin matrix and is unable to surround itself with other water molecules.

At room temperature, a water molecule is hydrogen bonded, on the average, to three other water molecules in a pseudotetrahedral structure (7, 8). In the resin phase, however, the resins ions, both fixed and mobile, orient the water

molecules about themselves and the matrix confines the internal water to capillaries, or pools, where at least one dimension is on the order of tens of Angstroms. Therefore the resin phase is weaker in its rejection of large ions and molecules than the external water phase.

Second, the structure of water has a tendency to force large weakly hydrated ions together to share one cavity in the water structure. Thus the water structure forces an ion pairing between a large ion and the resin, thereby yielding a selectivity which increases with increasing ion size.

Ion-Water

All ions have a tendency to attract and orient dipolar water molecules about themselves. This hydration process spreads the charge on an ion over a larger volume and lowers the free energy of the system. Highly hydrated ions tend to be small and highly charged. These ions will be preferred in the aqueous phase since their energy of hydration is lost when they are transferred to the resin phase. Larger, less hydrated ions such as cesium or potassium possess smaller amounts of hydration energy which are also lost on entering the resin phase. Therefore small highly charged ions such

as scandium or thorium tend to push the less hydrated ions into the resin phase in order to achieve maximum hydration in the aqueous phase (7, 8).

Ion-Ion

An ion can lower its electrostatic free energy by attracting ions of the opposite sign. This cation-anion complexing can stabilize these ions in either phase. This effect becomes increasingly important in concentrated solutions such as the resin phase where the effective dielectric constant is lower than in a dilute aqueous phase.

Ion-Resin Matrix

These interactions are the result of dispersion forces acting between large ions and the hydrocarbon matrix. These forces are usually small in comparison to the other interactions discussed.

From these interactions, a qualitative description of selectivity can be made. Selectivity is looked upon as the competitive solvating (by the aqueous coion, the resin fixed ion, and the water molecules in each phase) of exchanging ions where the ion with the smaller solvation requirements is pushed into the phase with weaker solvating properties.

The resin's preferential uptake of higher valence ions in dilute aqueous solutions ($Th^{+4} > Sc^{+3} > Ba^{+2} > Cs^{+1}$) can

be explained either by the Donnan potential (9) or by solvation needs (6, 7, 8).

The Donnan potential is an important factor in the exchange process. It occurs because one of the ions is fixed in the resin phase and is unable to diffuse into the aqueous solution. Since the resin-phase is usually more concentrated (for example: Dowex HCR-W, a cation resin has a capacity of 2.0 equivalents per liter in the sodium form and Dowex SBR-P, an anion resin, 1.3 equivalents per liter of resin in the chloride form) than the water phase, the resin's counterions (counterions are mobile ions with charges of the opposite sign of the fixed charges in the resin matrix. Coions are mobile ions of the same charge) tend to diffuse out to minimize the concentration differences in both phases. Also, for this reason the aqueous coions tend to move toward the resin phase. However this condition disturbs the electroneutrality of the two phases. A potential difference is formed at the water-resin interface which tends to repel coions and exclude them from the resin phase while at the same time attracting counterions. The magnitude of the water-resin interfacial potential depends upon the concentration difference between the two phases. The greater the dilution, the greater the potential. Additionally, since the force of attraction is also proportional to the

valence, higher valence ions are preferred by the resin phase.

If the solvating properties for each phase are looked at, it is seen that the higher valence ions can lower their free energy move by being in a concentrated solution where the effective dielectric constant is lower. Thus for a system with a dilute aqueous phase, the higher valence ions prefer the resin phase.

In order to simplify the description of the ion exchange selectivity process, in general only the behavior of tracer ions is considered. In dilute solution, resin invasion by macroelectrolyte is small and anion-cation interactions can usually be neglected. However the effects of the ion-water and the water-water interactions are important.

The distribution coefficient

$$D_A = \left[\overline{A}\right] / \left[A\right] \qquad (6)$$

is a useful quantity in tracer analysis. It is a measure of how strongly an ion is held by the resin. When combined with selectivity coefficient, $K_{A/B}$, the expression

$$D_A = \frac{\left[\bar{B}\right]^{|a/b|}}{\left[B\right]^{|a/b|}} K_{A/B}^{|1/b|}$$

$$= \frac{\left[\bar{B}\right]^{|a/b|}}{\left[B\right]^{|a/b|}} \cdot \frac{\gamma_A \bar{\gamma}_B^{|a/b|}}{\bar{\gamma}_A \gamma_B^{|a/b|}} Q_{A/B}^{|1/b|} \qquad (7)$$

is obtained. In dilute aqueous solutions, the aqueous phase activity-coefficient ratio is essentially constant, resin invasion is negligible, and the concentration in the resin is effectively equal to the number of resin sites per unit volume. Under these conditions the ratio of the resin-phase activity coefficients is also a constant and D_A is proportional to $\left[B\right]^{-|a/b|}$

$$D_A \propto \left[B\right]^{-|a/b|} \qquad (8)$$

The distribution coefficient displays the properties of the mass action effect in showing the relationship between the concentration of the eluting ion, B, and the valences of the two ions. In addition, comparison of the distribution coefficients of two ions would indicate the relative affinity for the resin these ions would display and, in turn, the relative ease with which elution would occur.

Table 1 contains values of distribution coefficients for selected elements at different HCl concentrations (4).

Table 1

Distribution Coefficients of Metal Ions on Dowex 50 x 8 Cation Exchange Resin in HCl Solution of Different Concentrations

Metal Ion	HCl Normality			
	0.1	0.5	1.0	2.0
Th^{+4}	$>10^5$	$\sim 10^5$	2049	239
La^{+3}	$>10^5$	2480	265	48
Ba^{+2}	$>10^4$	590	127	36
Al^{+3}	8200	318	60.8	12.5
Fe^{+3}	9000	225	34.45	5.2
Cr^{+3}	1130	73	26.69	7.9
Co^{+2}	1650	72	21.29	6.7
Cs^{+1}	182	44	19.41	10.4
Sr^{+2}	4700	217	60.2	17.8
Ni^{+2}	1600	70	21.85	7.2
Cu^{2+}	1510	65	17.5	4.3
K^{+1}	106	29	13.87	7.4

If anion selectivity is considered first, it is noted that the most common anions, excluding OH^- and F^-, do not possess a primary hydration shell and hence do not have strong ion-water interactions. As these interactions do occur, however, to some extent, the anions are able to interact more in the aqueous phase than in the resin phase leading to a situation where both exchanging anions prefer the aqueous phase. The smaller or more highly charged anion will be able to push the larger anion into the resin phase. Further, once there, the larger anions are pushed into a water-structure enforced ion pairing with the resin's quaternary groups.

For monatomic ions, the hydration requirements are inversely correlated to ionic size so that fluoride, whose ionic size is 1.3A^o, has stronger interactions with water than iodide, whose ionic size is 2.2A^o, and will be preferred in the aqueous phase.

Considering dilute solution cation selectivity next, there is a shift in the relative emphasis for the various interactions. The monatomic cations of a specified charge are a great deal smaller than the corresponding anions thus hydration plays a much larger role in the competition for the ions between the phases. Although the fixed resin ions is better able to interact as a solvating agent than the quaternary ammonium group of anion-exchange resins,

the hydration shell of the cation is not removed as it enters the resin. Hence the ion pairing, which occurs in anion exchange, is prevented.

In concentrated solutions, the selectivity is determined by the same interactions as in dilute solutions. The predominate effect, however, is no longer the hydration of the ions, but the complexing of the ion, by either the coion or the resin ion, and the partial destruction of the water structure (6, 7, 8). Other effects such as electrolytic invasion of the resin due to the falling Donnan potential also occur but are, in general, secondary.

These are the factors which determine the selectivity. It is important to understand how experimental conditions can affect the selectivity and hence the amount of eluant required for elution.

CHAPTER III

EXPERIMENTAL PROCEDURE

3.1 Experimental Apparatus

The description of the experimental apparatus is divided into several sections. A flow diagram, Figure 1, is provided to aid in visualizing the experimental configuration.

3.1.1 Pure Water Section

Tap water was distilled, collected, and stored in commercial 5 gallon plastic water containers. When needed, this water was pumped by a finger, or positive action, pump through two Barnstead mixed resin ion exchange cartridges to a 5 gallon polyethylene bottle located about 10 feet above the laboratory floor.

The deionized water leaving the cartridges had an electrical resistance greater than 2 megohms-cm as measured by a Solu Conductivity Bridge. This deionized water was used either as a wash liquid for the resin or for analytical purposes. Gravity provided the driving force for flow.

3.1.2 Elutriant Mixing and Storage

The solution used for elution was prepared in a 9 gallon pyrex tank and pumped to another 5 gallon

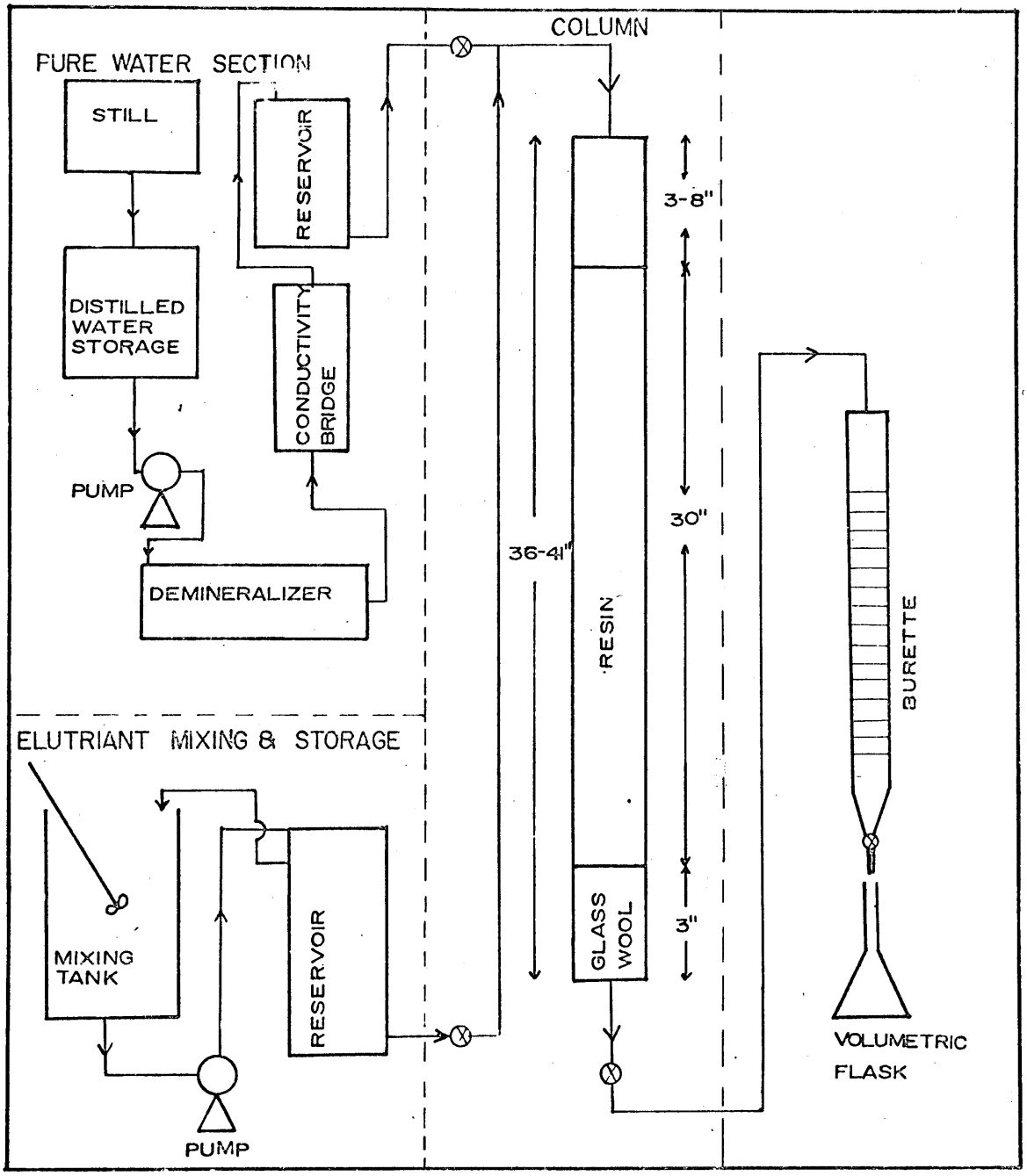

Figure 1 Experimental flow diagram

polyethylene bottle also 10 feet above the laboratory floor. Excess fluid was returned by a tube to the mixing tank to assure a constant head was maintained.

3.1.3 Column

Initially, a pyrex column was used during the sodium chloride elution experiments. However, to reduce the hazard of breakage, a plastic column of the same dimensions was used for all subsequent runs. The resin column length was 30.0 inches, the diameter was 7/8 inches, and the volumes were 298 cc and 304 cc for the pyrex and plastic columns respectively.

The resin was supported on a glass wool plug. During resin loading, the column was shaken and deionized water flowed down through the column until the settled resin height was 30.0 $\pm$ 1/4 inches.

During the 75°C elevated temperature runs, heating tapes were wrapped around the resin section and the liquid section above the resin. The heated section above the resin was used to preheat the incoming liquid to the desired operating temperature while the resin section was heated to maintain a constant temperature ($\pm$ 3°C) along the length of the column. The temperature measurements were made with thermometers located at both ends of the resin section.

3.1.4 Flow Measurement

The flow was measured by the length of time needed to collect a known effluent volume. A 25 ml burette at the column exit and a timer facilitated the flow rate measurement. The burette also served as a holding tank while volumetric flasks, used to collect the effluent, were changed. The flow stability was ± 10% in the range 1/4 - 2 gpm/ft^2.

3.2 Procedure

As only monobed (one resin type) experiments were performed to avoid the necessity of any elution of metal ion-macroelectrolyte anion complexes, the resin in either the sodium or chloride form was placed in the column. The column was vibrated during resin loading and washing to promote settling of the resin phase until a constant height of 30 inches was achieved. Using dilute solutions of the test ions (0.24N), the resin was "trace loaded" (approximately 1 %) and then washed with deionized water. The wash effluent was collected and analyzed for any test ion leakage. Following this, the elutuant was fed into the column at a predetermined flow rate. When the interface between the descending elutriant and the wash water came in contact with the exchange resin, collection of the effluent was initiated. These effluent samples were later analyzed for the counterion plus the test ion(s) using the procedures outlined in Appendix B.

3.3 Variables

Table 2 is a summary of the experimental parameters and the range over which they were varied. Initially pH was also investigated but, since many higher valence metal ions such as thorium, ferric iron, bismuth, aluminum, and zirconium form insoluble hydroxides in slightly acidic ($pH > 4$) solutions, it was decided to use a pH that was sufficiently low to prevent hydrolysis of most ions ($pH = 1.5$).

3.4 Selection of Test Ions

3.4.1 Test Ions

A specific ion in each valence grouping was selected as a test ion. This was done primarily on the basis of the equilibrium data of Nelson, Maurase, and Kraus (18, 19) for ion exchange of elemental ions in HCl and $HClO_4$ solutions. The test ions chosen were cesium (+1), barium (+2), scandium (+3), thorium (+4), and iodide (-1).

3.4.2 Selection Criteria

To represent each valence group, the ion selected was the most tightly held by an exchanger. Because these ions were the most tightly held, they provided "boundary" conditions for each valence group.

If ions, other than the test ions, were present on an exchanger to be processed, the amount of eluant required would then be less.

Table 2

Experimental Conditions Studied

VARIABLE	RANGE
Test Ions	Valences: -1 to +4; ions: iodide, cesium, barium, scandium, and thorium
Elution Agents	Ferric chloride, ferric sulfate, sodium chloride, and sodium sulfate
Elutriant Concentration	0.13 - 1.97N
Flow Rates	1/4 - 2 gpm/ft^2
Temperature	Room temperature and 75°C
pH	1.5

The elution of the test ion defines the maximal amount of elutriant needed for complete elution of its valence group. This also explains why these ions were chosen over ions, such as cobalt-58, which are of interest to designers of radioactive waste disposal systems.

3.4.3 Importance of Thorium Selection

In the tetravalence group, thorium was chosen as the test ion and was of particular interest for two reasons. First, thorium is the most tightly held cation, regardless of valence group, on strong-acid type cation exchange resins. Since thorium is more tightly held than other elements like uranium [$D_{Th} > 10^5$ and $D_U > 10^2$ at 0.5M HCl (18)], which will be found on the reactor's exchange resin, the elution of thorium provides an indication of the maximum amount of elutriant needed for complete elution of the resin.

Secondly, thorium has an extremely low diffusion coefficient in the resin phase [$2.15 \cdot 10^{-10}$ $cm^2 \cdot sec^{-1}$ at 25°C for Dowex 50x8 (21)]. Hence diffusion kinetics play an extremely important role in the elution of thorium. Other monatomic cations have diffusion coefficients which are, in general, larger than that of thorium (21, 23, 5).

Due to these two factors, the elution of thorium presents more difficulties than that of other ions. For a specific set of operating conditions, thorium will pro-

vide either kinetic and/or equilibrium limitations on the elution more severe than on other ions. Thus, the elution of thorium could be called the "worst possible case" since it would require the maximal amount of eluant for a specific set of operating conditions.

3.5 Neutral Salts As Eluting Agents

3.5.1 Selection of Elutriants

The initial criteria for selection of the eluting salt to be studied were availability, ease of handling, economy, and high density. Sodium chloride was the first investigated.

The ineffectiveness of sodium chloride as an eluting agent (see Discussion of Results, Thorium) caused additional criteria to be added to the initial criteria. These were that the eluting cation possess a high affinity for the resin, which can be measured by its distribution coefficient for hydrogen, the eluting anion possibly complexes cations thus aiding the cation resin elution, and that the eluting anion have a strong affinity for the anion resin (to eliminate a possible multisalt process).

Under these criteria, ferric salts were selected for further investigation. The ferric ion had an additional advantage. It possesses a low distribution coefficient (< 1) for the cation resin in 3 - 4 M HCl solutions due to anionic complexing. Thus the ferric ion could easily

be removed if the cation resin were to be reused.

Both ferric chloride and ferric sulfate were investigated. The advantages of using ferric sulfate over ferric chloride in a commercial process were several: the salt would be easier to process than the chloride (ferric sulfate would have a lower vapor pressure and would be less corrosive than ferric chloride) and the sulfate ion would complex the higher valence cations more effectively (12, 27). However several metals, primarily the alkaline earths form a precipitate with sulfate. The literature (13) indicated that the elution difficulties engendered by this precipitation could be alleviated by careful choice of the elutriant concentration and the flow rate. Experimentally, the precipitation problem did occur for barium and ferric chloride was used with better results.

Ferric salts were unsuitable for use in the anionic resin elution. The ferric ion oxidizes the iodide which deposits in the resin as iodine.

$$2\ Fe^{+3} + 2I^{-} \rightleftharpoons 2Fe^{+2} + I_2 \qquad (9)$$

Alkali metal salts were investigated for the iodide elution. Of the common anions, sulfate has the highest preference for the strong base anion resin phase. Sodium sulfate was used as the anionic eluting agent.

3.5.2 Physical Properties of Eluting Agents

Table 3 lists the physical properties (24, 25, 26) that will be useful in the evaluation of the eluting agent effectiveness. These selected properties are the salt form after the solvent has been evaporated and the crystal density at ambient conditions.

3.6 Resin

3.6.1 Resin Properties

The resins used in the experiment were Dowex HCR-W and Dowex SBR-P. The physical properties (14, 15) of each are listed in Table 4.

3.6.2 Resin Form

It was decided to study the elution characteristics of the exchange resins (either the cation exchange Dowex HCR-W or the anion exchanger Dowex SBR-P), when they were initially in the sodium or chloride form respectively.

3.6.3 Resin Form Justification

As part of the water purification system in water-cooled nuclear reactors, ion exchangers are used in either the hydrogen or alkali metal form for the cation exchanger and in the hydroxyl form for the anion resin. The resins are not exhausted prior to removal from the coolant system, they are still primarily in these forms. Use of resins in these forms or in forms where the main

Table 3

Density and Hydration Number of Elution Agents

Salt	Hydration Number at 100°C	Crystal Density at 25°C of 100°C Form
NaCl	0	2.16
Na_2SO_4	0	2.7
$FeCl_3$	0	2.9
$Fe_2(SO_4)_3$	2	2.7

Table 4

Physical Properties of the Resin

Property/Resin	Dowex HCR-W	Dowex SBR-P
Type	strong acid cation	strong base anion
Crosslinking (%)	8	not defined
Specific Gravity	1.28 (Na form)	1.07 (Cl form)
Capacity (meq./ml. wet resin)	2.0 (Na form)	1.3 (Cl form)
Void Volume gal/ft^3	3	3
Maximum Operating Temperature (^oF)	300	140 (OH form) 300 (Cl form)
Effective pH range	0-14	0-14
Sphericity (%) Minimum	95	90
Standard Mesh Size (wet)	20 - 40	16 - 40
Pressure Drop (psi/ft of resin depth $W=20 gpm/ft^2$, $T=75^oF$)	1	1.4

components distribution coefficient is not too different from the reactor form utilized allows a "practical process" problem to be modelled. As exchangers in the sodium or chloride form fulfill this requirement, it was decided to use the resins in these forms, as supplied by the manufacturer.

3.6.4 Resin Loading

In every elution run, six milliequivalents of a test ion were loaded on the column. This corresponded to a loading of 1% for the cation resin and 1.5% for the anion resin, each column having a volume of about 300 cc. Trace loading was used for two reasons. First, it modelled the true situation in reactor resins and second the diffusion of the trace ion is reported to be the rate-controlling step (10, 11). This latter effect can be seen, if it is realized that in a trace component system the individual diffusion coefficients, the activity coefficients, the degree of swelling, etc. remain practically constant and the coupled diffusion constant, $\bar{D}_{AB}$, is effectively that of the trace component (22).

The elution of thorium and iodine was run separately while the cesium, barium and scandium runs were done simultaneously.

3.6.5 Loading Distribution

The test ions were loaded in a band at the top of the resin column.

CHAPTER IV

DISCUSSION OF RESULTS

A summary of elution conditions plus typical elution data can be found in Appendix A. Several of the graphs have "equivalents of iron" as an abscissa, if "bed equivalents of iron" is desired instead, the abscissa value should be divided by 0.6 since each cation resin bed had a capacity of 0.6 equivalents of exchange capacity.

It should be noted that the differential elution curves were plotted starting with the first effluent sample which contained either eluting agent or test ion.

4.1 Thorium

The elution of thorium was studied as a function of the flow rate and the concentration of the eluting agent. Figure 2 is an example of thorium elution as a function of effluent volume and exhibits behaviour characteristic of the thorium-ferric sulfate system which is the appearance of thorium prior to the breakthrough of iron. Also exhibited is an exponential decrease of the effluent's thorium content as a function of solution volume (or amount of iron) after the iron concentration in the effluent equals that of the inlet.

Figures 3, 4, and 5 plot the amount of thorium

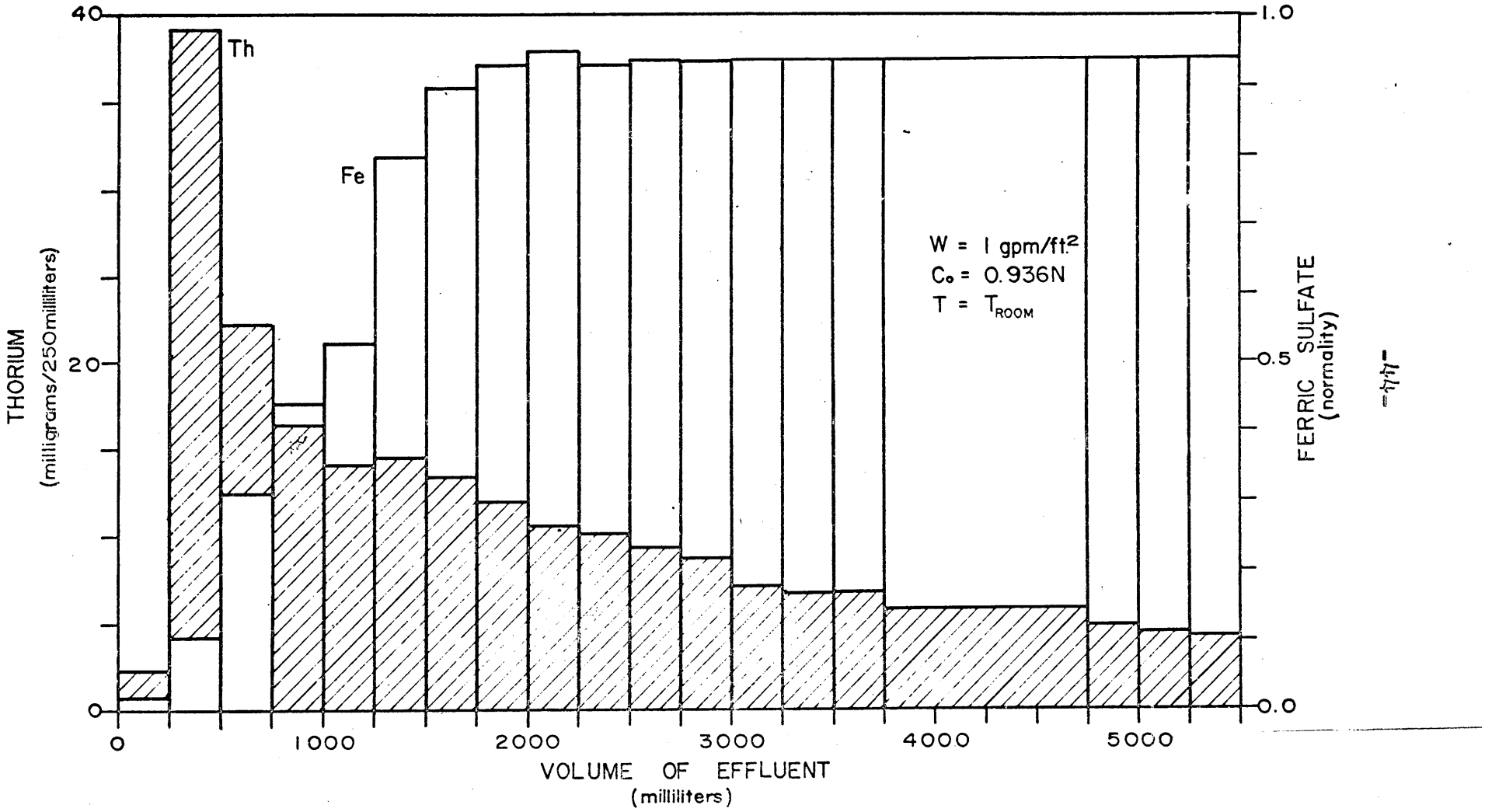

Figure 2 Plot of ferric sulfate and thorium concentrations versus effluent volume.

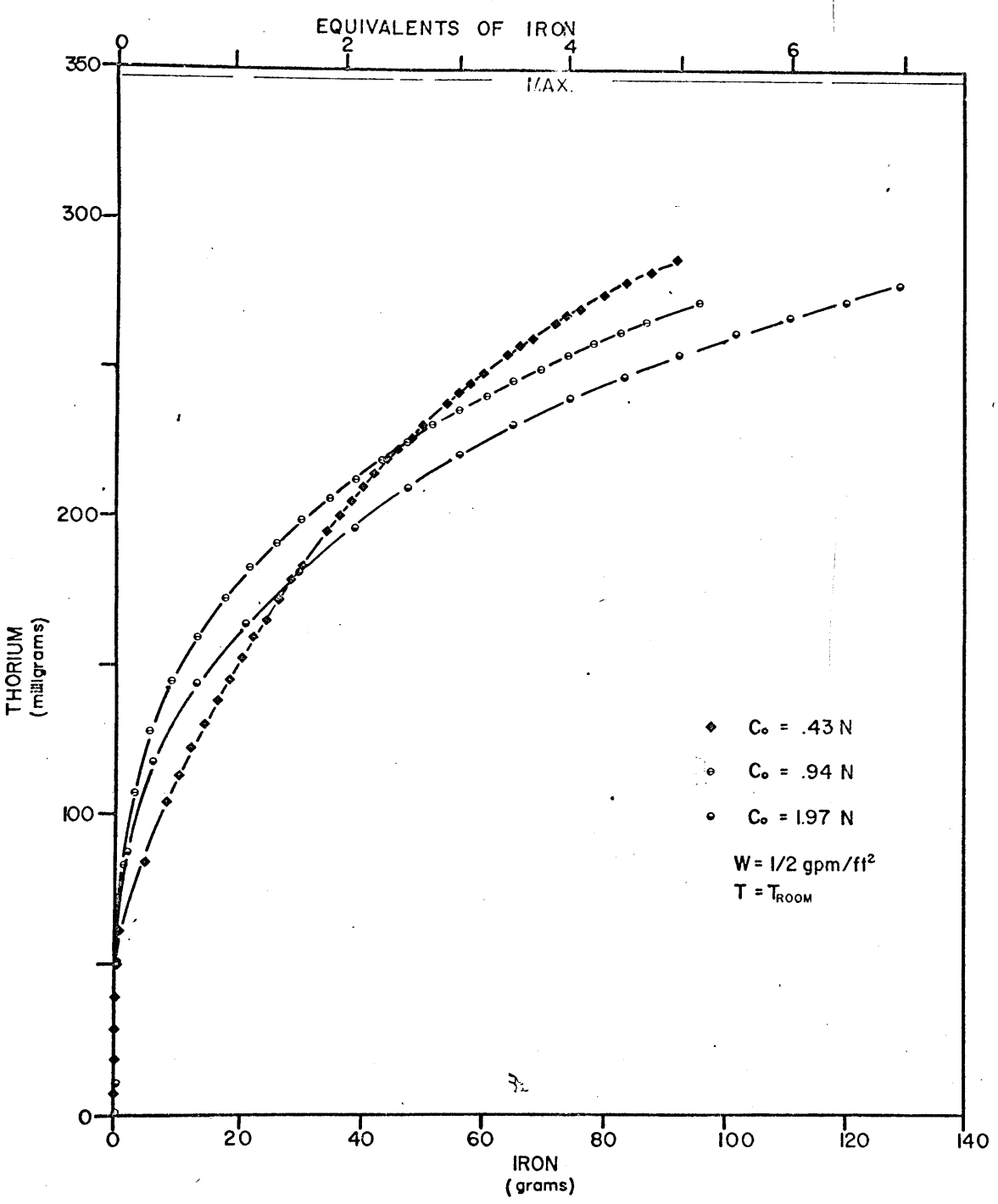

Figure 3 Plot of the effect of ferric sulfate concentration on thorium elution

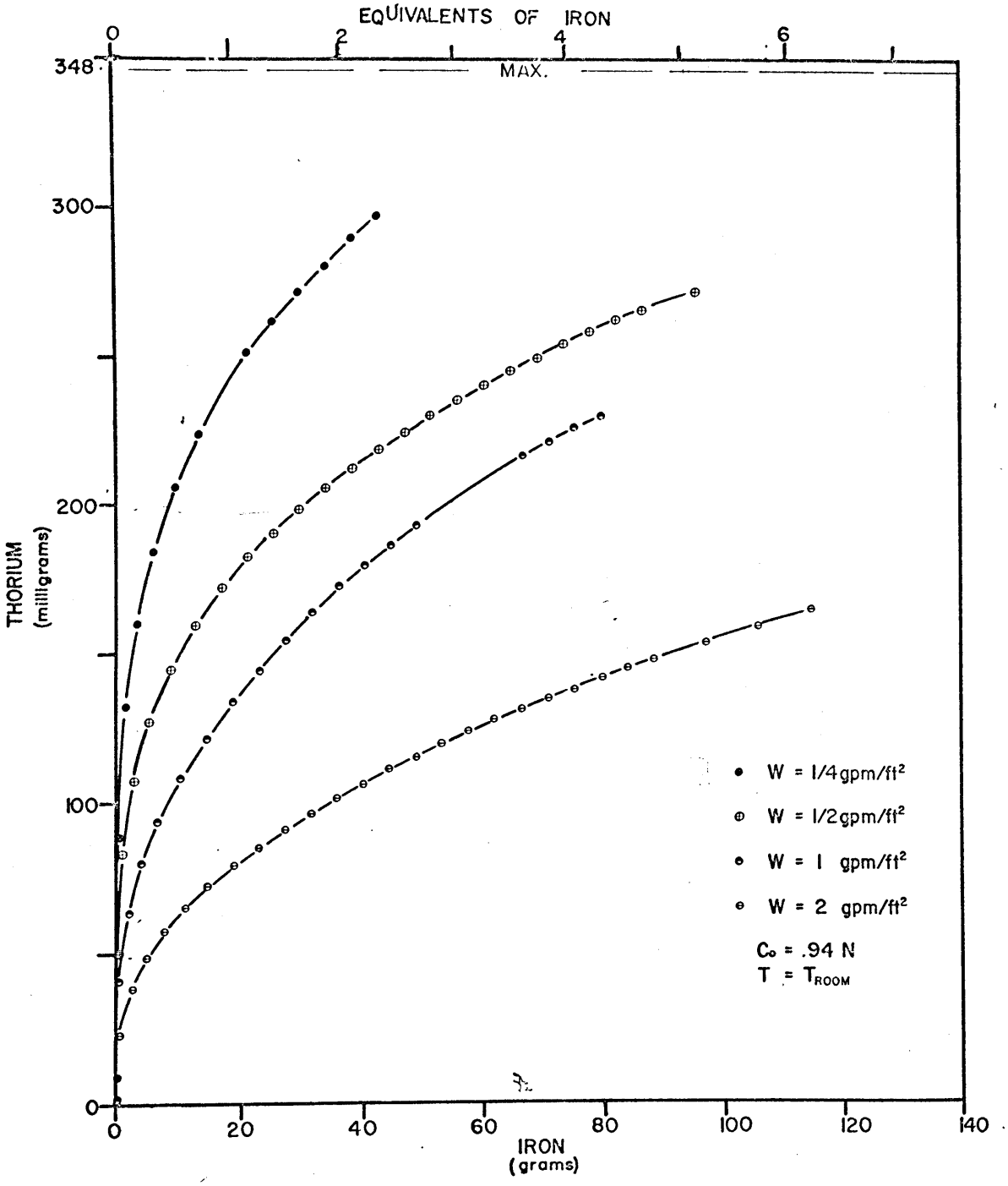

Figure 4 Plot of the effect of flow rate on thorium elution by ferric sulfate

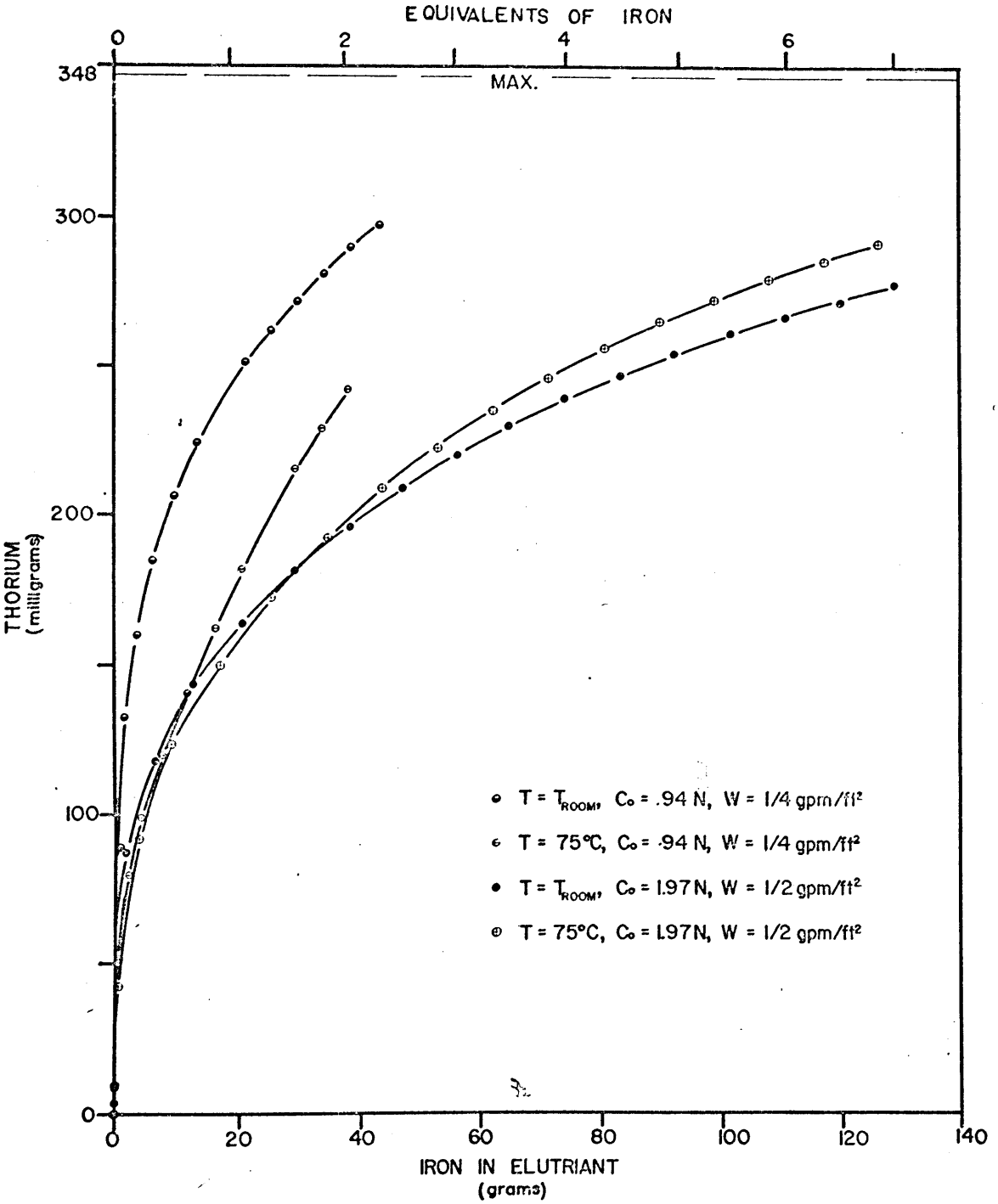

Figure 5 Plot of the effect of temperature on thorium elution under various conditions

eluted from a constant loading of 1% as a function of the amount of iron in the effluent. Figures 6, 7, and 8 plot the same data but in the form of the fraction of thorium remaining on the column instead of thorium eluted. The parameters varied are flow rate, concentration, and temperature.

In Figures 6 through 8, after the iron concentration of the effluent equals that of the inlet, the thorium data lies on straight lines, with slopes α, as if the elution were occurring in a well-stirred flow system instead of being eluted in a band as it was loaded.

Initially the slope of these curves changes very rapidly; this transient is probably due to the high free sulfate concentration which is present from the resin's absorption of the ferric ion. At the column inlet, the free sulfate is only about 1/3 of the total sulfate in solution, with the remainder complexing the iron (12).

$$Fe^{+3} + SO_4^{-2} \rightleftharpoons FeSO_4^{+} \qquad K_{25^oC} = 104 \qquad (10)$$

As the solution procedes down the column, the iron is exchanged for the sodium and thorium on the resin. The free sulfate concentration increases (sodium does not form complexes with sulfate) and drives the thorium complexing (12)

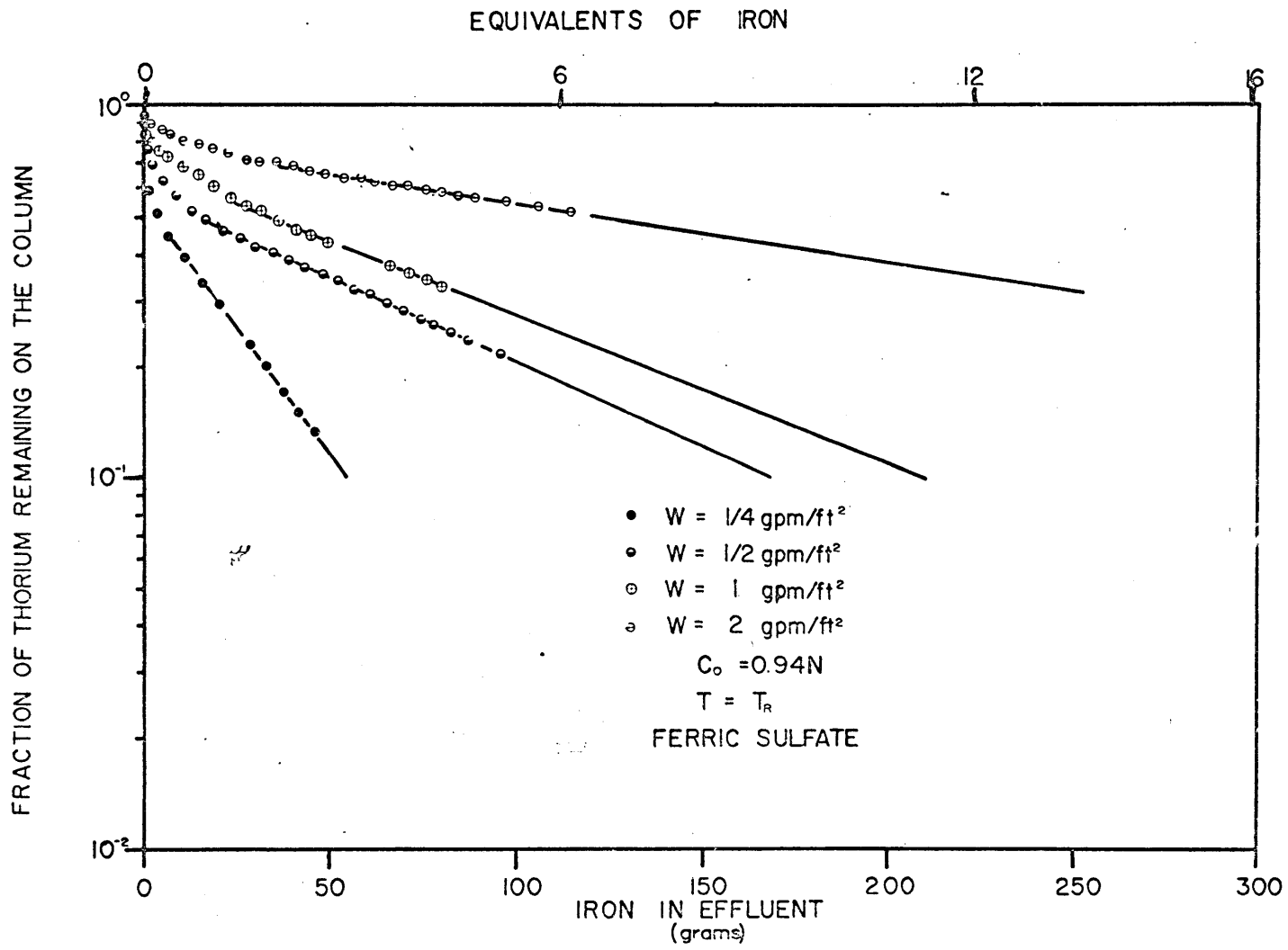

Figure 6 Plot of the fraction of thorium remaining on the column resin versus iron in the effluent as a function of flow rate for C_o =0.94N, T = T_R, and ferric sulfate.

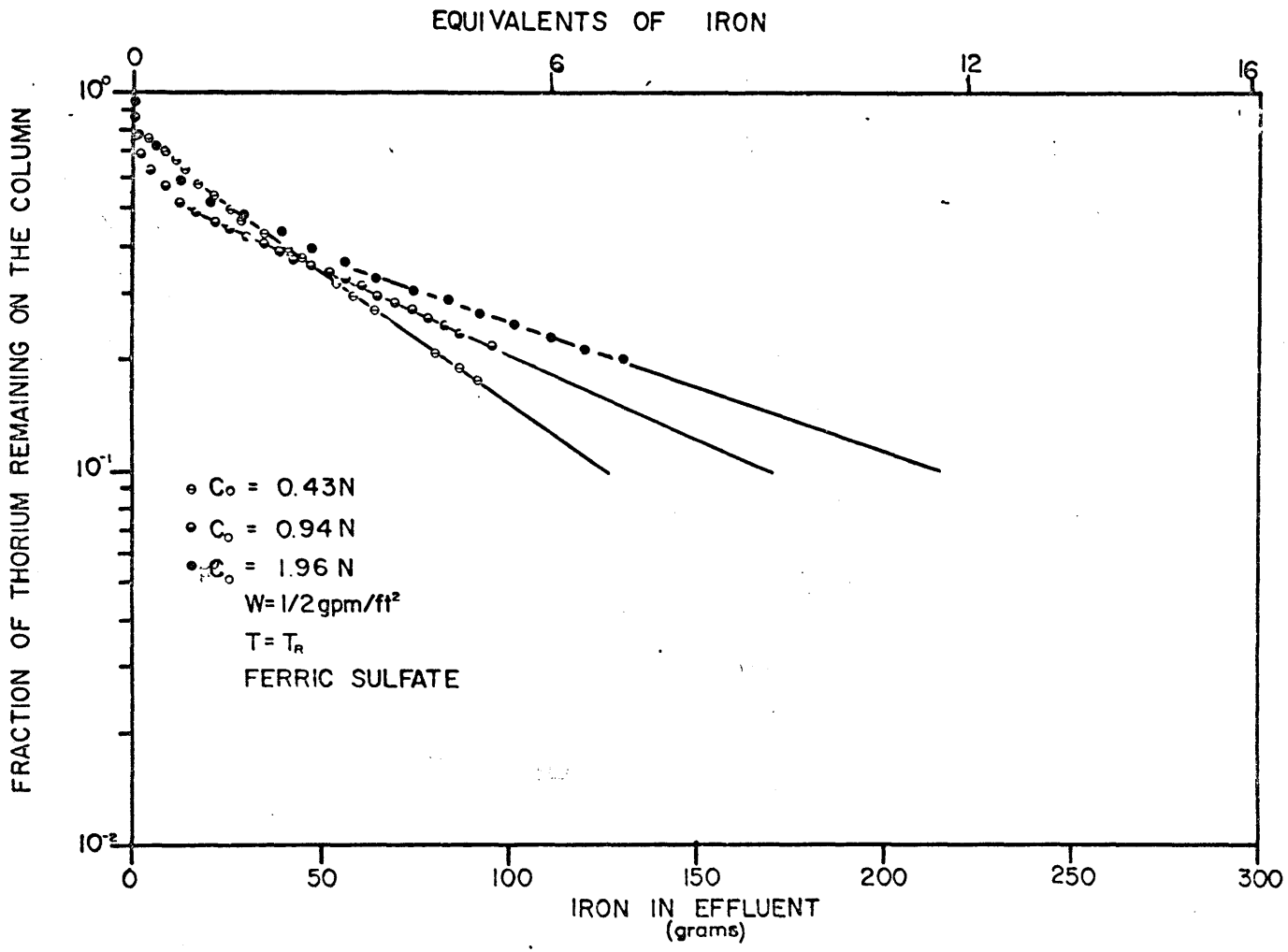

Figure 7 Plot of the fraction of thorium remaining on the column resin versus iron in the effluent as a function of concentration for W = 1/2 gpm/ft², T = T_R, and ferric sulfate.

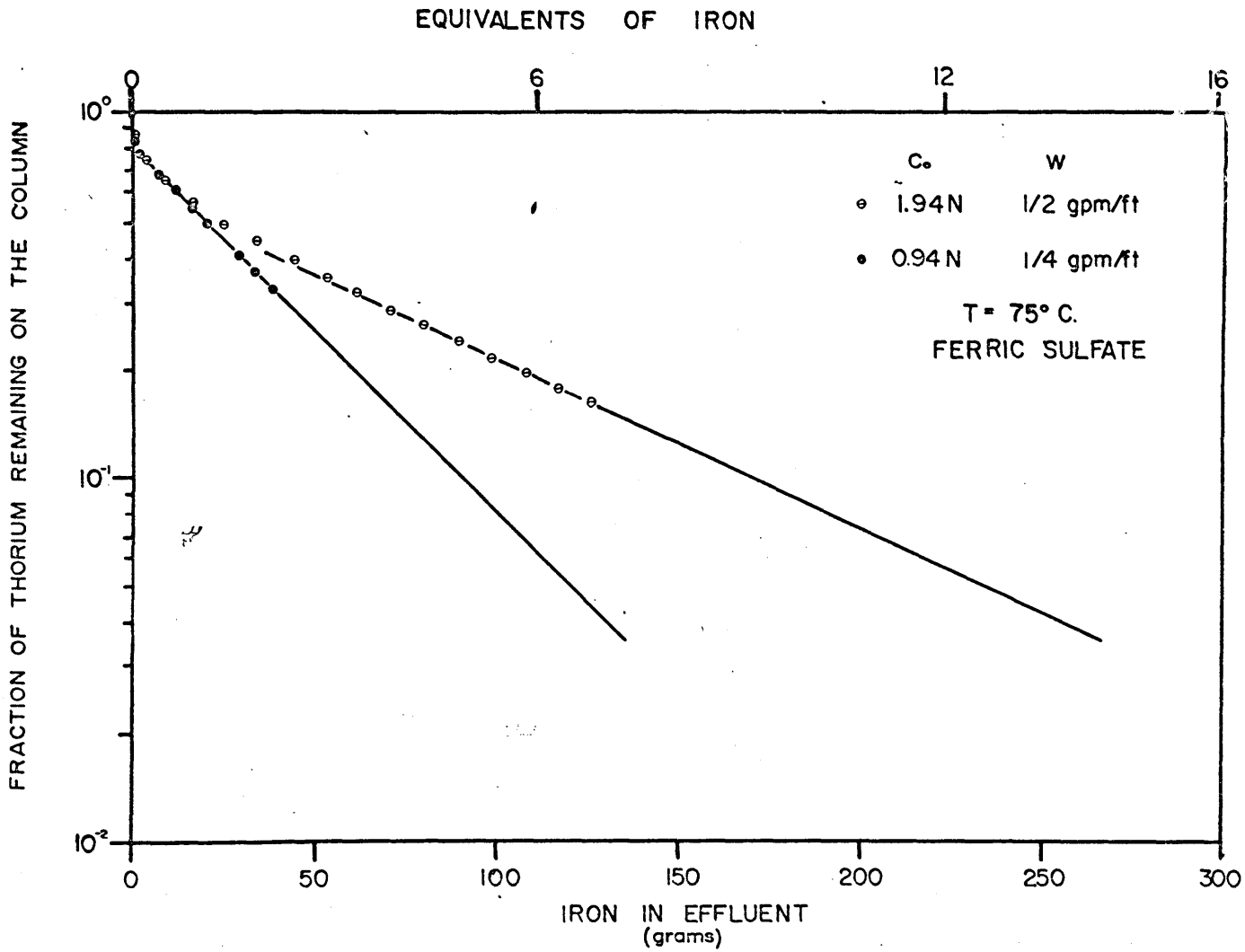

Figure 8 Plot of the fraction of thorium remaining on the column resin versus iron in the effluent at T = 75°C. for different flow rates and ferric sulfate concentrations.

$$Th^{+4} + 2SO_4^{-2} \rightleftharpoons Th(SO_4)_2 \qquad K_{25°C} = 10^{5.6} \tag{11}$$

further to the right [formation of anionic complexes can also occur (27)] . If the amount of thorium complexing increases, the uncomplexed thorium concentration in solution drops. It is this uncomplexed concentration which enters into the equilibrium expression, Equation (4), and into the rate expression

$$\frac{\partial N_i}{\partial t} = \beta(n_i - n_i') \tag{12}$$

n_i is the non-equilibrium concentration of exchangeable ion, i, in solution; mequivalents per unit column length

N_i is the corresponding non-equilibrium concentration in the resin, unit as n_i

t is time

β is the effective rate constant for sorption of the exchanging ions, and

n_i' is the equilibrium concentration of the ion in solution

for the diffusion of thorium from the resin. Decreasing the uncomplexed concentration causes the driving forces for mass transfer (and consequently its rate) to increase. This increased rate of mass transfer combined with the varying free sulfate concentration present in the initial stages of the elution causes the rapidly changing slope

in the beginning of each elution with ferric sulfate.

The low diffusion coefficient of thorium in the resin phase tends to support this kinetics-limited view since long contact times would be required for equilibrium to be closely approached. However it is the variation in the effective use of the iron, for a constant iron concentration, as a function of flow rate, see Figure 4 or 6, which shows conclusively that the elution of thorium is kinetic and not equilibrium controlled.

Figure 6 is a plot of the fraction of thorium left on the column versus iron in the effluent for a constant iron concentration. It shows the dramatic decrease in the amount of iron needed for elution when slow flow rates are used. Slow flow rates permit a longer contact time between the two phases and hence allow a closer approach to equilibrium. However there is a flow rate below which the effective use of the iron will only marginally improve the elution due to the close approach to equilibrium. This limiting flow rate was not determined and it might be the objective of some future research or obtained from engineering performance data.

The effect of temperature on the elution was studied, Figures 5 and 8. It was expected that an elevated temperature would increase the diffusional rate and offer better utilization of iron through a closer approach to equilibrium.

The equilibrium constant for ion exchange is known not to have a strong temperature dependence (28). Thus it was expected that the thorium elution curve for elevated temperatures would be above that at ambient temperatures, all other parameters being the same. However this did not occur, see Figure 5. Instead the initial portion of the elevated temperature runs were below those at ambient temperatures indicating thorium was more rapidly eluted at ambient temperatures than at 75°C. As the elution curves continued, however, the 75°C runs either cross or are about to cross the corresponding room temperature elution curves.

It is felt that the probable explanation to this "crossover" behaviour, although it was not proven, was a strong temperature dependence of the complexing equilibria, Equation (11). If the equilibrium constant for complex formation is significantly decreased, the initial elution efficiency or iron utilization will be greatly decreased. As the effluent iron approaches that of the inlet, the diffusional rate increase will begin to predominate. This increased rate of mass transfer will eventually cause the crossover of the higher temperature run over that at ambient temperatures. Increasing the elutriant concentration would be expected to cause a reduction in the magnitude of the temperature effect. This would be due to the

larger value for the free sulfate concentration which would tend to increase complexing. This is demonstrated in the two sets of runs in Figure 5 where the difference between the elevated and the room temperature runs at high inlet concentrations is smaller than those made at lower concentrations.

Figure 9 plots the slopes, α , for the linear portion of the elution curves in Figures 6 and 7 as a function of flow rate and concentration. α is a measure of the mass transfer coefficient, β , and the distribution coefficient, D_{Th}. It is a measure of the rate at which thorium is transferred from the resin phase to that of the solution, Equation (12). Inspection of the values of α shown in Figure 9, for a constant iron concentration (0.94N), shows a 9 fold variation in α for an 8 fold variation in flow rate (1/4 - 2 gpm/ft^2). If thorium is eluted at a rate proportional to the amount present on the resin, the variation in α would be 8 fold in going from 2 to 1/4 gpm/ft^2 since the iron in the effluent per unit time is proportional to the flow rate. The experimental value for the α variation is in good agreement with this idea.

The variation of α for different iron concentrations and constant flow rate can be explained this way also, since the amount of iron through the column per unit time is proportional to concentration. A 2.1 variation in corresponds to a 4.5 variation in concentration. This

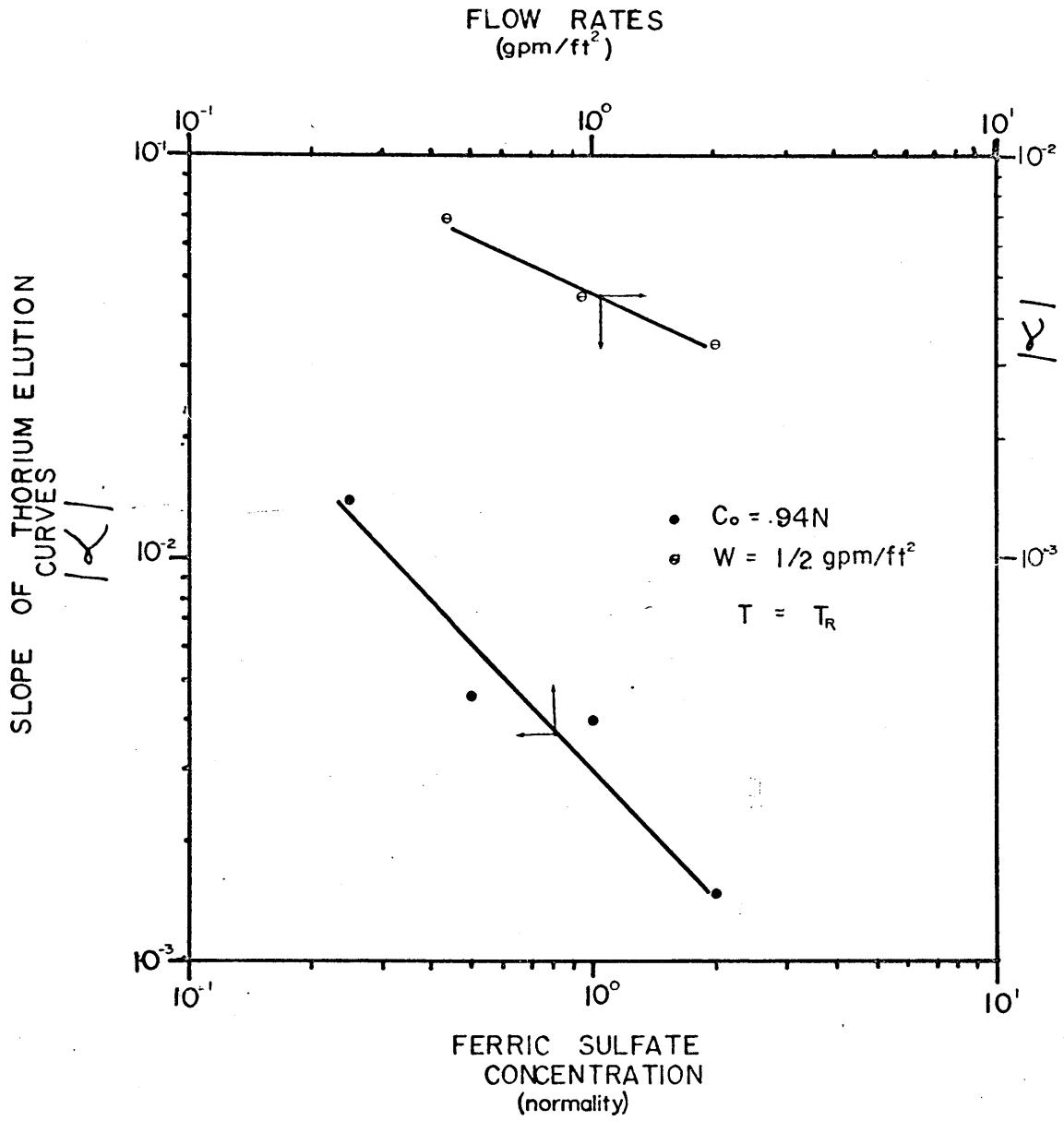

Figure 9 Plots of thorium elution slopes versus iron concentrations and flow rates.

apparent discrepancy is explained by considering the mass action effect for the uncomplexed iron in addition to the amount of iron in the effluent per unit time. Varying the concentration will affect the mass transfer coefficient, β, slightly; however the equilibrium concentration of thorium in solution, n'_{Th}, will be affected due to the mass action effect. All other conditions remaining constant, a 4.5 variation in eluant concentration (this corresponds to a 1.7 variation in the uncomplexed iron concentration Equation (10).

$$\frac{[Fe\ SO_4^+]}{[Fe^{+3}]\ [SO_4^{-2}]} = \frac{[y]}{[d-y][e-y]} = 104 \qquad (10a)$$

where

y = molar concentration of the iron complex, m./l/

d = the total iron molar concentration m./l.

e = total sulfate molar concentration, m./l.

For an eluant concentration of 0.43 N and 1.97 N, the uncomplexed iron concentrations are 0.012M and 0.02M respectively.) will cause a 2.0 variation in n'_{Th} and the mass transfer rate. Dividing the 4.5 variation in concentration (or iron through the column per unit time) by the 2.0 variation in the mass transfer rate leads to an expected variation in α of 2.25 which again is in good agreement with experiment.

The linear dependence of α on concentration and flow rate indicates that there is not a close approach to equilibrium for the conditions studied. This is indicated since it appears that the driving force in the mass transfer relation, Equation (12), is primarily the equilibrium concentration of thorium in solution, n'_{Th}. It is assumed that particle diffusion is rate-controlling in this elution, the half-time of the exchange reaction can be approximated in an infinite solution from a knowledge of the resin bead's radius and the internal diffusion coefficient in the resin (22).

$$t_{1/2} = 0.030 \frac{r_o^2}{\bar{D}} \qquad (13)$$

Thus the rate of exchange is proportional to the diffusion coefficient, $\bar{D}$, in the exchanger and inversely proportional to the square of the bead radius. For thorium this corresponds to a half-life of about 100 hours. If the flow rate were adjusted such that the residence time of the elutriant in a 3 ft resin section was equal to this, a flow rate of about 0.001 gpm/ft^2 would be required. However, since axial diffusion at this low flow rate plays a major role and since most metal ions have diffusion coefficients larger than thorium, a flow rate of 0.01 gpm/ft^2 is recommended for a commercial elution step.

Experimentally the best operating condition for the elution of thorium using ferric sulfate as eluate was at Co = .94N, W = 1/4 gpm/ft^2, and T = T_{ROOM}. For a 90% removal of thorium, see Figure 6, from the column, 54 grams of iron would be in the effluent. This corresponds to a $Fe_2(SO_4)_3 - 2H_2O$ residual salt volume of 78 cc or 25.6% of the cation resin volume. Since 600 mequivalents of iron were exchanged for sodium in the first part of the elution, the total amount of iron used in the elution was 65.1 grams. This corresponds to an inlet solution volume of 12.4 cubic feet of solution per cubic foot of cation exchanger.

Improvement on this elution performance can be made using an extremely low flow rate (such as .01 gpm/ft^2), ambient temperature, and an eluant concentration greater than 1N. (Increasing the concentration above 1N would involve the possibility of even further reductions in flow rate).

Figure 10 is a check on the reproducibility of the data under identical operating conditions (C=0.94N, W=1/4 gpm/ft^2). As can be seen, the agreement between the data of the two runs is good.

The elution of thorium by sodium chloride was extremely inefficient. Figure 11 is the case where the entire resin bed was saturated with thorium (for analytical

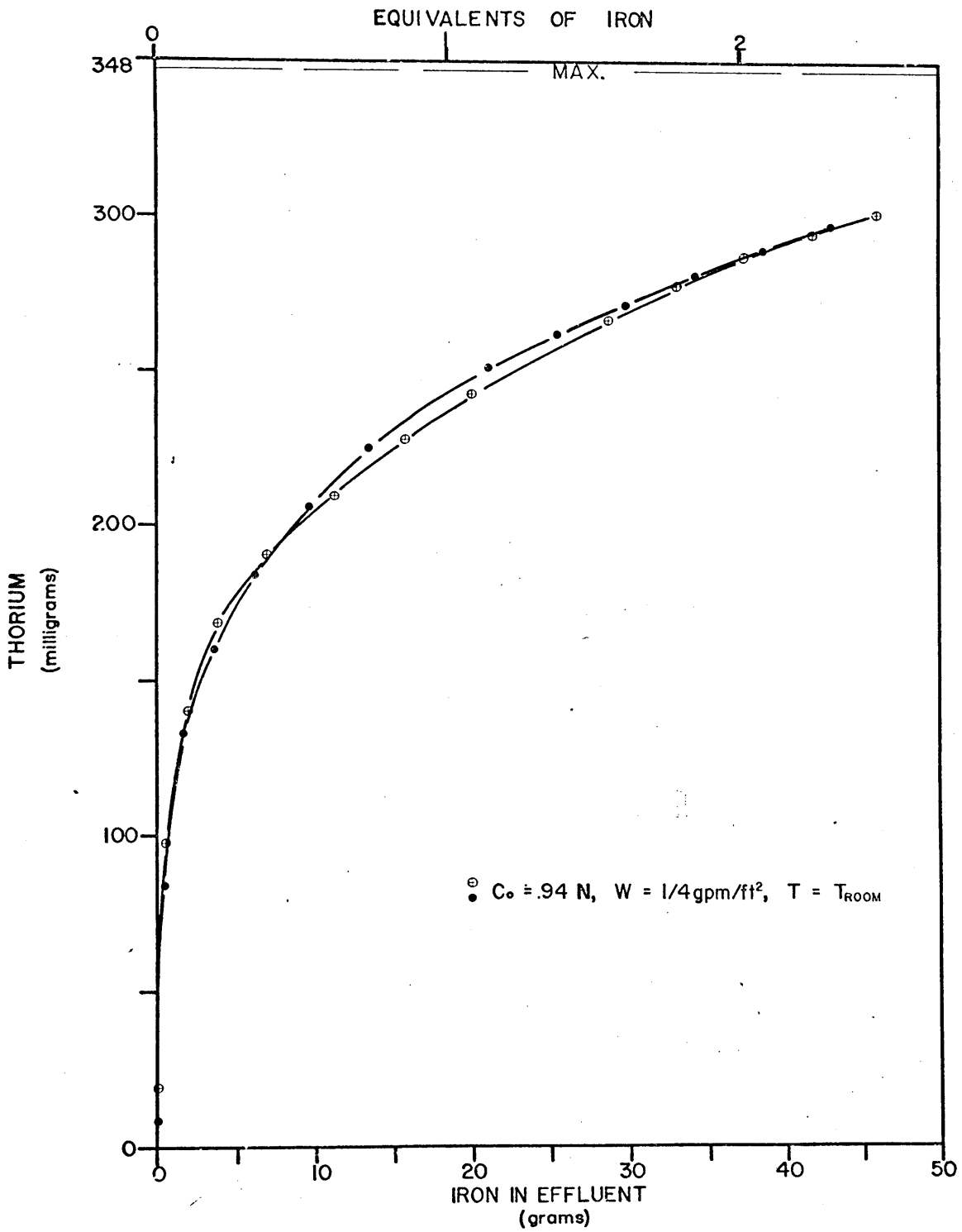

Figure 10 Plot demonstrating experimental reproducibility

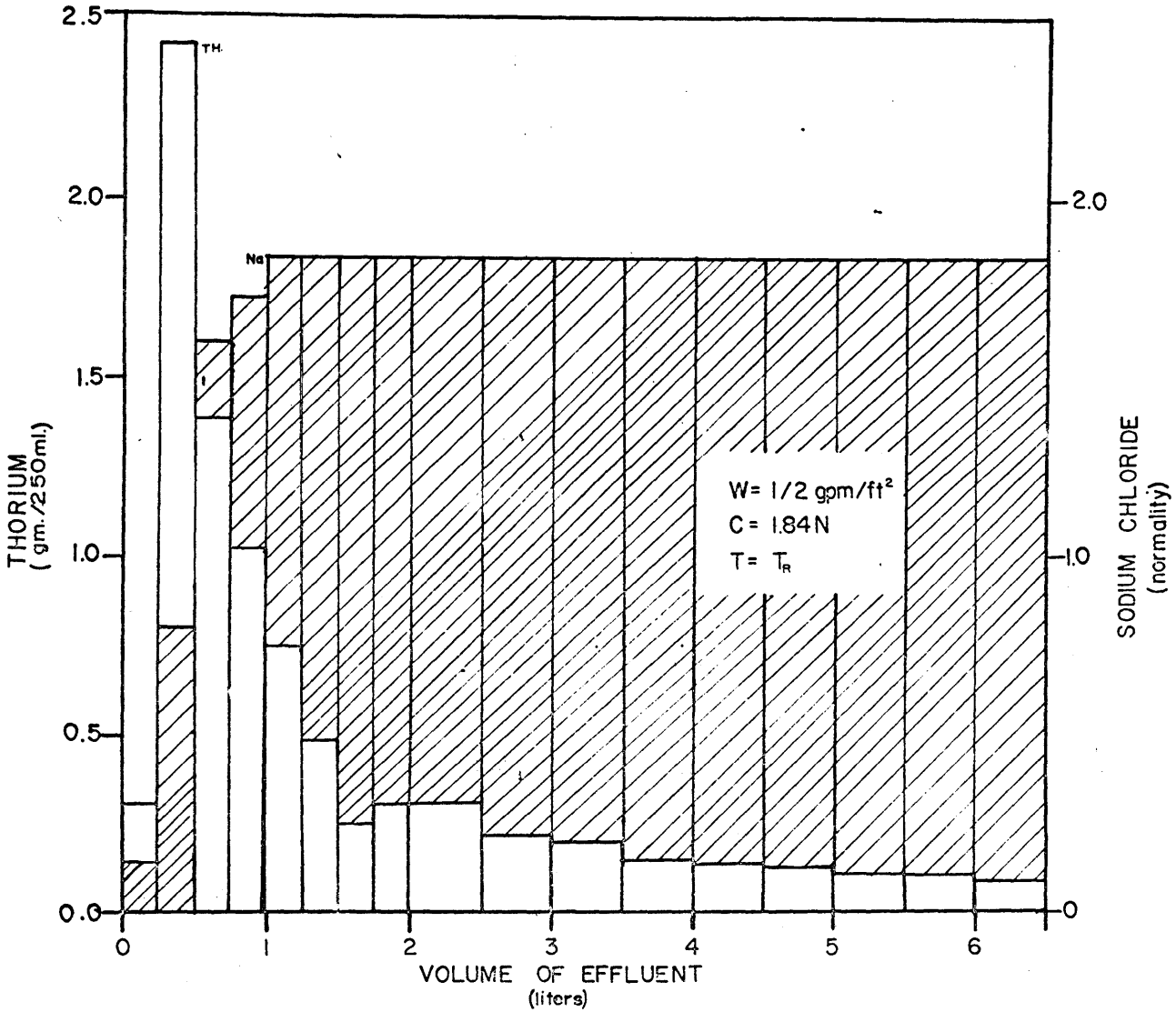

Figure II Elution of thorium from an initially competely loaded resin using sodium chloride as elutriant

reasons) prior to elution. For 300 cc of dry sodium chloride, which equals one column volume of resin, only 28% of the thorium was eluted. Since the distribution coefficient of a component decreases with increasing loading of that component (29, 30), a greater fraction of the thorium was eluted for the saturated loading than if the thorium had been a trace component.

4.2 Scandium

With ferric sulfate as the eluting agent, scandium follows the same general elution behaviour, Figure 12, as thorium, Figure 2. In this graph the fractions of scandium eluted per unit volume and iron concentration in the effluent are plotted versus the volume of effluent leaving the column. As with thorium, 6 mequivalents of scandium was loaded onto the resin.

Figures 13 and 14 contain the scandium elution data. Figure 13 relates the total amount of scandium eluted while Figure 14 the fraction scandium remaining on the resin as a function of iron in the effluent for different flow rates, concentrations, and eluting agents.

In these two figures, one curve (eluting agent: $Fe_2(SO_4)_3$; Co = .36N; W= 1gpm/ft^2) shows a sharp discontinuity. Experimentally, the break was initiated by a partial flow blockage which was discovered and eliminated after one sample volume. However, for unknown reasons

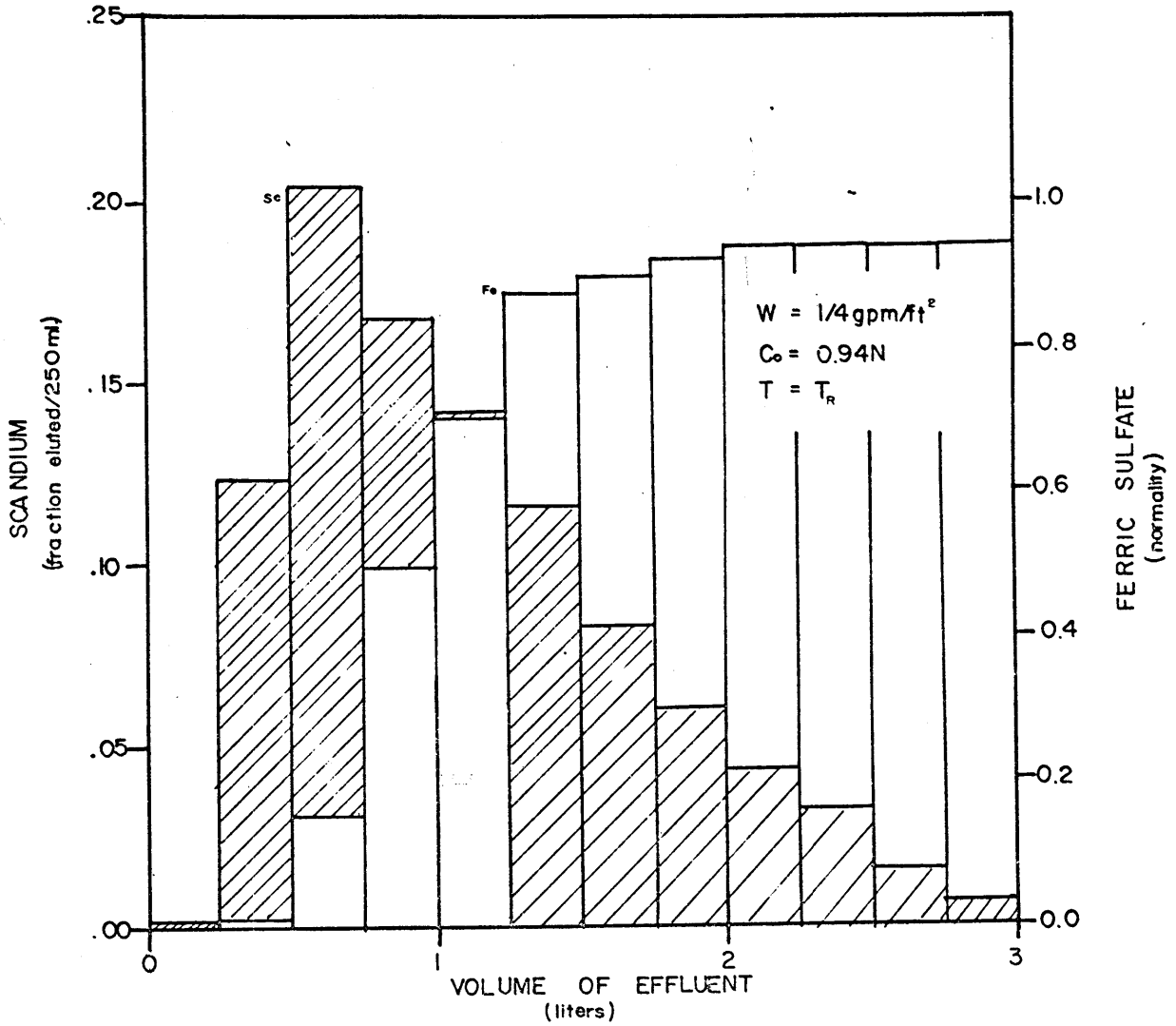

Figure 12 Plot of ferric sulfate and scandium concentrations versus effluent volume

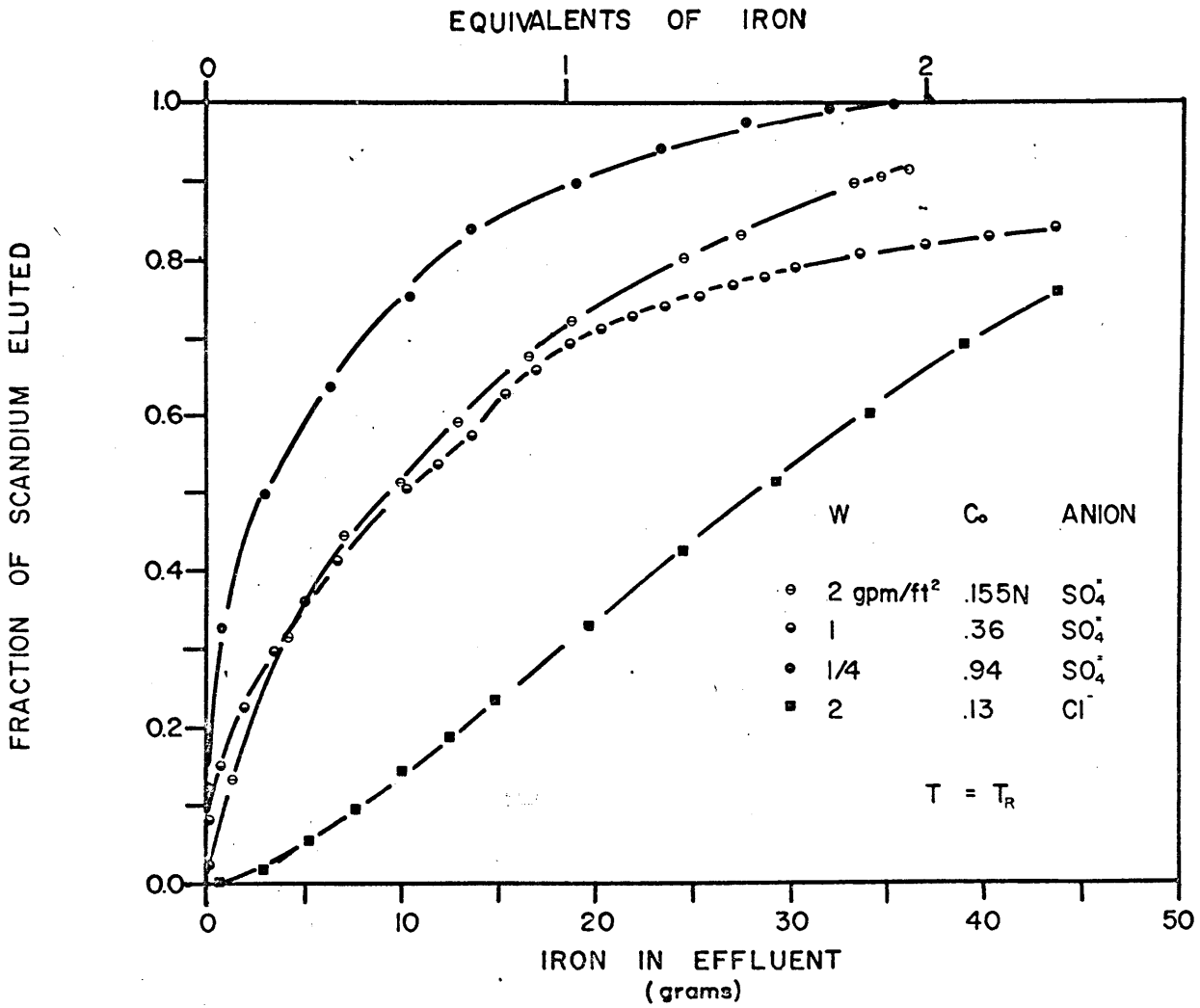

Figure 13 Elution of scandium for varying flow rates, ferric concentrations, and anions at constant temperature

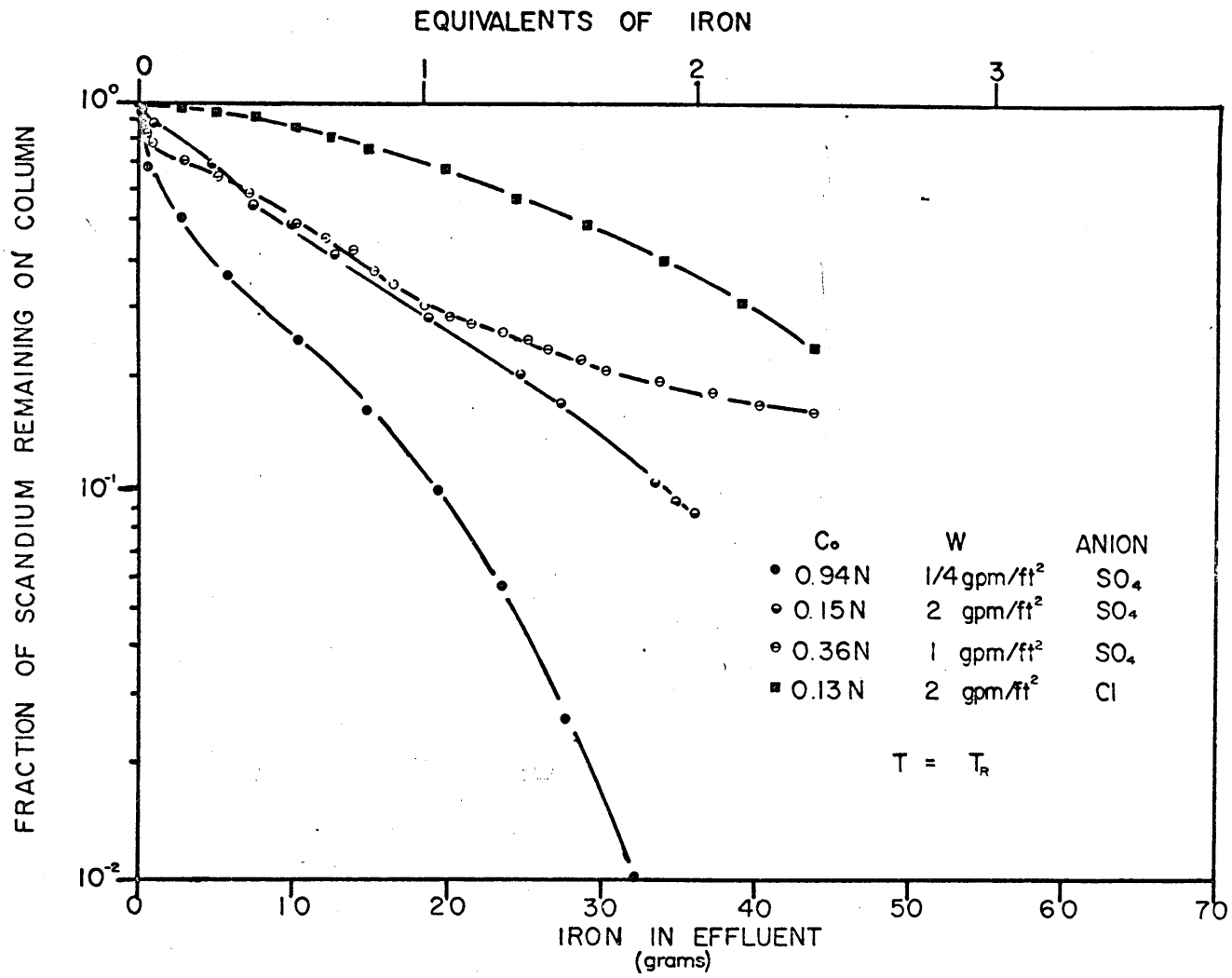

Figure 14 Plot of the fraction of scandium remaining on the column resin versus iron in the effluent for different elution conditions at $T = T_R$.

the curve continued to deviate after correction of this difficulty. Prior to this break, the elution was similar to one made at about half the salt concentration (0.154N) and twice the flow rate (2 gpm/ft^2) emphasizing again the importance of contact time (about the same for these two cases per unit iron).

Comparison of the sulfate and chloride system curves show the effectiveness of using a complexing agent as sulfate to aid in the elution of heavy metal ions. In the ferric chloride system scandium is eluted in a band, Figure 15, while in the ferric sulfate system, a well-stirred flow system curve, Figure 12, similar to that of the thorium elution is followed.

From the "mass action law", Equation (5), the effective use of iron as an eluting agent for ions of the same valence should not depend on the elutriant concentration provided equilibrium is achieved. However, the concentration of the complexing anion should be as high as possible.

The same low flow rate, ambient temperature, and high ferric sulfate concentration is recommended for the scandium system's elution as that for the thorium's.

From the experimental data, the best operating condition was Co = .94N, W = 1/4 gpm/ft^2, T = T_{ROOM}, and the eluting agent-ferric sulfate. Under these conditions, 99% of the scandium was eluted with 32 grams of iron in

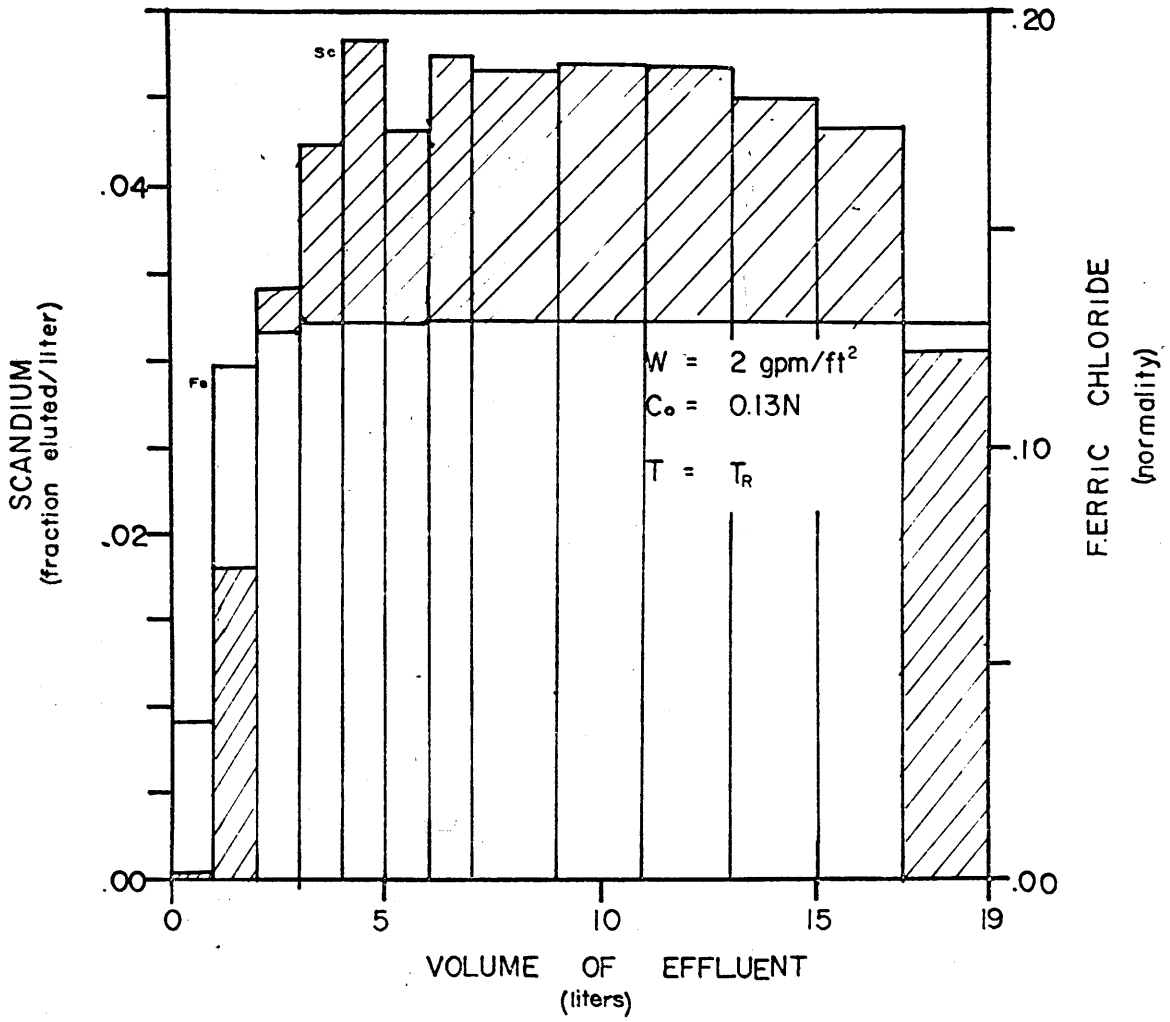

Figure 15 Plot of ferric chloride and scandium concentrations versus effluent volume

the effluent. This corresponds to a volume of 46.3 cc of doubly hydrated ferric sulfate or 15.3% of the cation resin volume.

As in the thorium calculation, addition of the amount of iron exchanged for the sodium to the amount of iron in the effluent requires an inlet volume of eluant of 8.2 cubic feet of solution per cubic foot of resin.

In all runs, scandium was loaded unto the resin together with barium and in all but one ($W = 1/4$ gpm/ft^2; $Co = .93N$; $T = T_{ROOM}$; ferric sulfate) with cesium, so that the elution of these three ions was studied simultaneously.

4.3 Barium

In the range of flow rates (1/4 - 2 gpm/ft^2) and concentrations of ferric sulfate (.15 - .94N) tried, precipitation of barium sulfate occurred. This precipitate was located in a narrow band at the top of the resin. However the formation of this precipitate did not seem to hinder the elution of cesium and scandium which were also located at the top of the column.

The elution of barium using ferric chloride, Figure 16, as an eluting agent was successful. As with the elution of scandium with ferric chloride, the barium was eluted in a band. Application of the "mass action law" to the case of elution by a higher valence ion indicated that the amount of iron needed for the elution at equilibrium would decrease

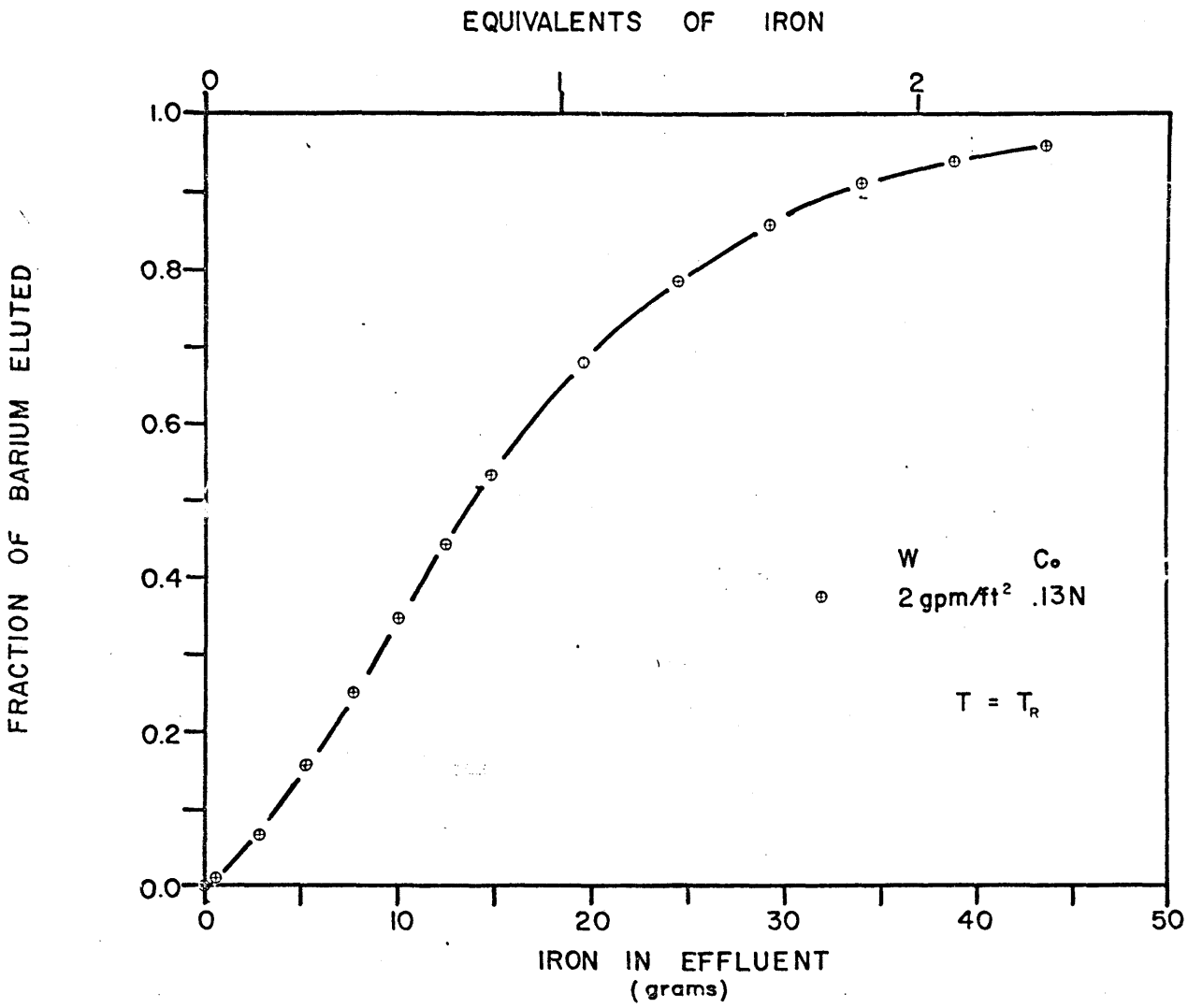

Figure 16 Elution of barium with ferric chloride

with decreasing ferric iron concentration.

For the experiment using ferric chloride as the eluting agent (Co = .13N; W = 2 gpm/ft^2; and T = T_{ROOM}), 96% of the barium is eluted for 43.7 grams of iron in the effluent. This corresponds to 45.5 cc of dried ferric chloride or 14.4% of the cation resin volume. In terms of the required input solution volume, there are 76.1 cubic feet of solution per cubic foot of resin.

The recommendations for a more effective use of the iron in the elution of barium involve using ferric chloride as the eluting agent at a concentration of about 0.13N and slow flow rates to insure a close approach to equilibrium. An exact flow rate can not be specified since the only value available is 2 gpm/ft^2, but, if Equation (13) is used with $\bar{D}_{Ba} = 3.3 \cdot 10^{-8}$ cm^2/sec (21), a flow rate of about 1/8 gpm/ft^2 for a 3 ft column would be a good starting place for the elution.

4.4 Cesium

The association of cesium with sulfate is small, thus cesium was eluted in a peak in both the ferric chloride and ferric sulfate systems, Figure 17. The utilization of iron improved with decreasing concentration of the elutriant, Figure 18. Elution of the alkali metals would be extremely efficient using dilute ferric salt solutions (< 0.15N). The flow rate did not seem to be as critical

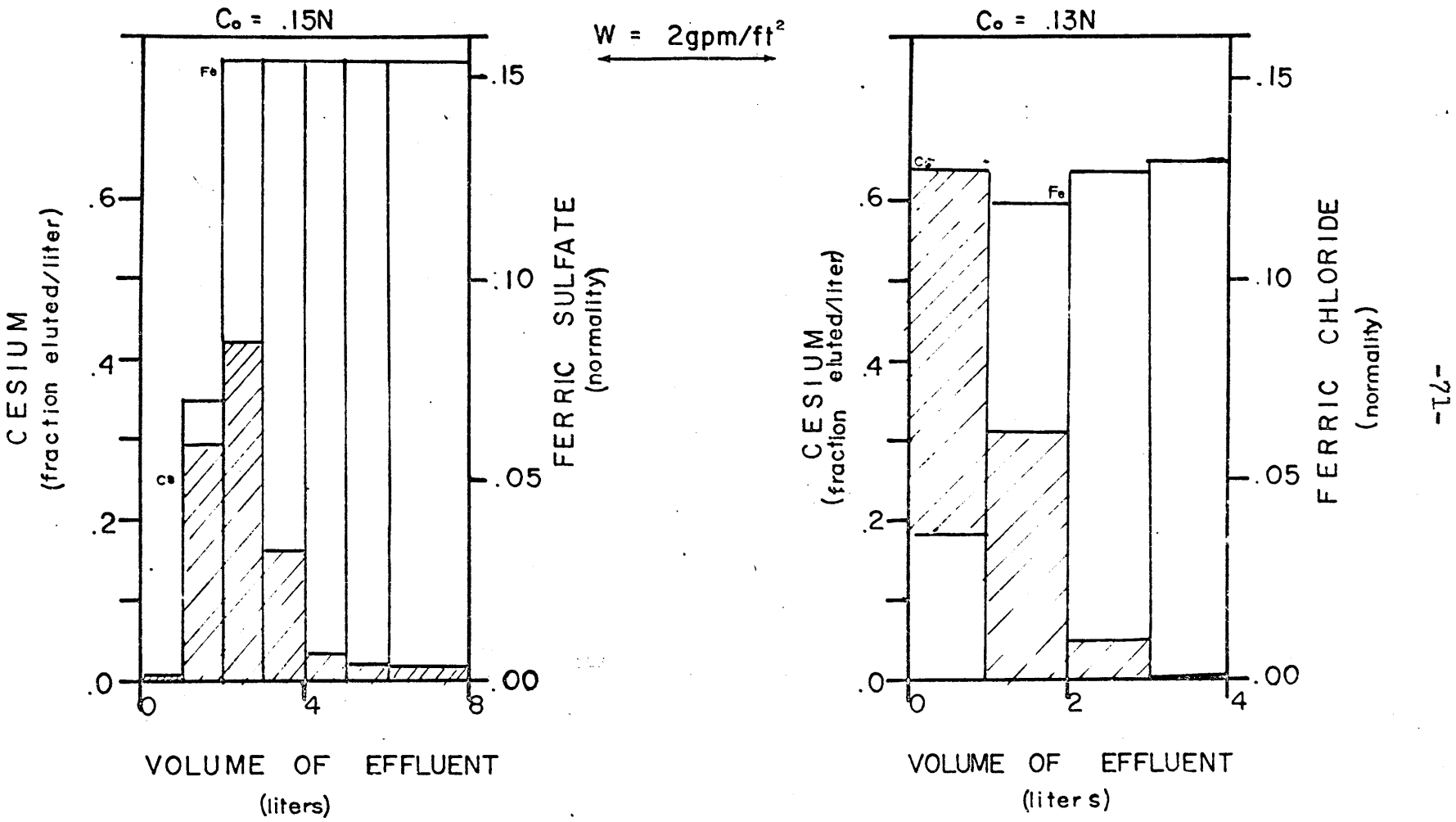

Figure 17 Plots of cesium and ferric sulfate/chloride concentrations versus effluent volume

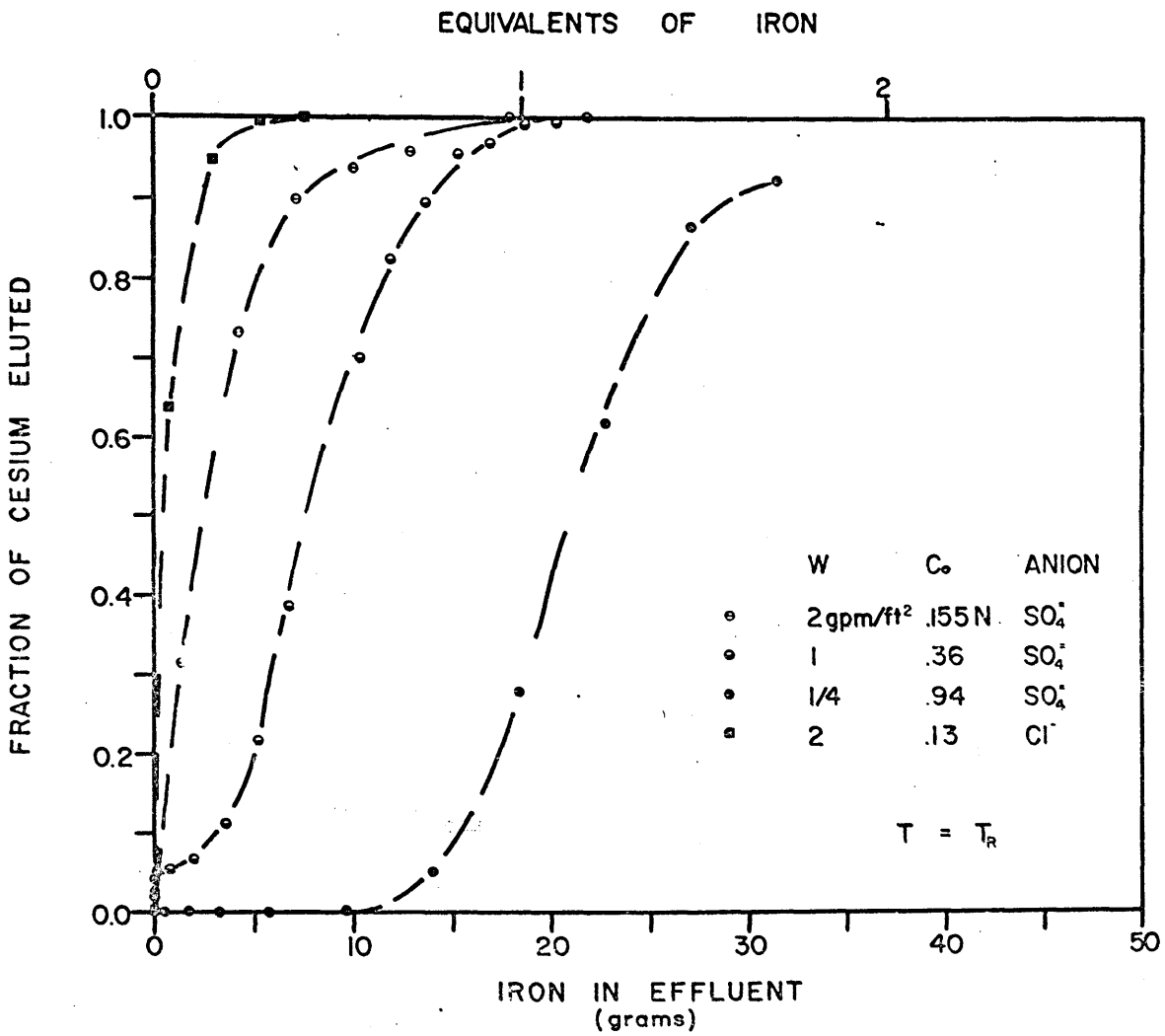

Figure 18 Elution of cesium for varying flow rates, ferric concentrations, and anions at constant temperature

a parameter for cesium elution as for higher valence ions.

The precipitation of barium did not seem to interfer with the elution of cesium. There was one experimental run without barium or scandium in the column (Co = .94N, W = 1/4 gpm/ft^2; T = T_{ROOM}, and ferric sulfate).

Experimentally the best operating conditions for the cesium elution occurred using ferric chloride as the eluting agent and operating conditions of Co = .13N, W = 2 gpm/ft^2, and T = T_{ROOM}. With 7.7 grams of iron in the effluent, all of the cesium was eluted for a residual ferric chloride volume of 8.0 cc or 2.6% of the cation resin volume. The volume of ferric chloride solution required for this elution was 25.9 cubic feet of solution per cubic foot of resin.

Although flow rate does not seem to be an important parameter for the univalent exchange group, the same conditions of operation for cesium as for barium are recommended.

4.5 Iodide

Ferric salts are unusable for this system due to the redox reaction, Equation (9), of the iodide and the ferric ions. This reaction occurred inside the resin bead where the deposited iodine was difficult to remove.

Sodium sulfate was used, Figure 19, and the elution exhibits chromatographic, or band, behaviour.

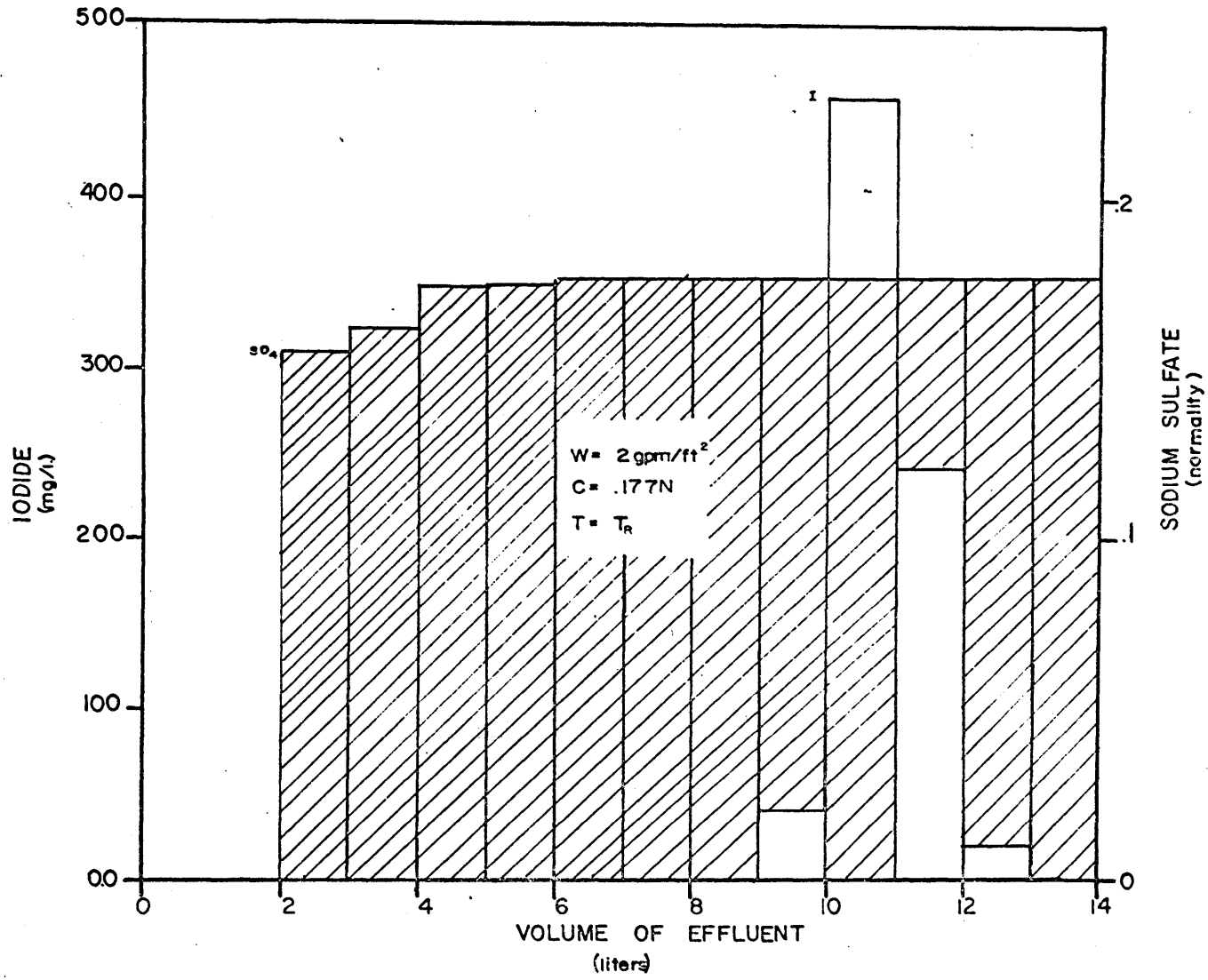

Figure 19 Elution of iodide using sodium sulfate as elutriant

In the elution experiment using sodium sulfate ($Co = .18N$, $W = 2$ gpm/ft^2, and $T = T_{ROOM}$), 91.3 grams of sulfate in the effluent were used for the complete removal of iodide from the anion resin. This corresponds residual volume of 16.4% of the anion resin volume. In terms of inlet solution volume, this corresponds to 113 cubic feet of solution per cubic foot of resin.

A more effective eluting agent is needed to reduce the volume of solution to be evaporated. Sodium nitrate might be an acceptable substitute. It could be used in a concentrated solution since there is no concentration effect on the efficiency of the exchange between ions of the same valence.

If sulfate is to be used, however, going to lower flow rates [such as 1/2 gpm/ft^2 using $\bar{D}_I = 1.33 \cdot 10^{-7}$ (21) and Equation (13)] would obtain slightly better elution of the iodide. Dilution of the elutriant would reduce the residual volume of salt. However the large resulting effluent volume may make this option undesirable due to the resulting high cost of evaporation.

CHAPTER V

APPLICABILITY OF RESULTS

5.1 Introduction

Normalization of the data presented in this study, to the conditions of an operational reactor resin, requires an evaluation of the importance of parameters not specifically investigated experimentally. The parameters involved are the resin loading, the initial ion distribution in the column, and the column dimensions.

Contaminated reactor resins are characterized by the following conditions:

1) trace loading of radioactive ions,

2) generally uniform distribution of the radioactive ions, and

3) column height or diameter can be arbitrarily fixed.

These parameters will be discussed separately under equilibrium elution conditions, since this provides the simplest limiting case, and then under non-equilibrium elution conditions.

5.2 Loading

Trace loading occurs when the equilibrium concentration of the microcomponent in the liquid is a linear function of its concentration in the resin. Carroll

(29, 30) has investigated the range of resin loading both theoretically and experimentally, and has shown that, at least for uni-multivalent exchange, the distribution coefficient varys slightly with resin loading until a substantial fraction of the resin is loaded { > 50% loading in the case of univalent (NO_3^-) - divalent $\left[Th(NO_3)_6^{2-} \right]$ exchange }.

For the range of resin loadings where the linear relationship or the case-exchange isotherm is of the form

$$\frac{N_1^{1/Z_1}}{N_2^{1/Z_2}} = k_{1,2} \frac{(n_1')^{1/Z_1}}{(n_2')^{1/Z_2}} \qquad (14)$$

$k_{1,2}$ is a constant for the exchange

$n_i'(i=1,2)$ is the respective equilibrium concentration in the solution phase in meguivalents per unit column length

$Z_i(i=1,2)$ charge on ion i

theoretical calculations (16, 31, 32, 33, 34, 35) have been made showing the independence of the volume of regenerating solution on the resin loading.

If, under equilibrium conditions, there are no factors blurring the front ("ideal" situation), a terminal or sharp regeneration-ion front moves along the column. The elutriant volume is independent of the exchange constant and depends only on the relative concentration of the

two phases (35).

The sharp front model is generally unrealistic and calculations are made assuming that the sorption kinetics are achieved under equilibrium conditions (34) with a slight initial blurring of the boundary. Under these conditions, the volume of the eluting solution needed for a complete regeneration is dependent upon the equilibrium constant and the ratio of the concentrations in both phases, is still independent of the loading.

If the exchange occurs between ions of different valences, there is an eluting solution concentration (for reasons such as solubility, this may not be attainable) at which the isotherm switches from a concave (or unfavorable equilibrium) to a convex (or favorable one) form. The equation describing the elution tends toward the "ideal" case (34). The limiting equations for the different equilibrium cases are:

"ideal"

$$V_R = V_0(\frac{1+h}{h}) \tag{15}$$

"equal" valence

$$V_R = V_0(1 + \frac{k_{1,2}}{h}) \tag{16}$$

"unequal" valence

$$V_R = V_0\left(1 + \frac{k_{1,2}^{Z_1}}{h^{Z_1/Z_2}}\right) \qquad (17)$$

$k_{1,2}$ constant for the exchange

V_R volume of regenerating solution needed for complete elution

V_0 void volume of the resin column

h the ratio of the equivalent concentration in the solution and in the resin phase in mequivalents per unit column length

$Z_i (i=1,2)$ valence of the eluted (i=1) and eluting (i=2) ion.

Experiments (16, 31, 33) conducted to test equations developed, in general, fit the data. There are small differences between the calculated and experimental elution volumes and these differences appear to be due to diffusional effects.

In summary loading is not a significant parameter in the range studied. Under these conditions, the amount of eluant required is independent of the degree of trace loadings.

5.3 Ion Distribution in the Column

When the test ions are loaded onto the column resin

in a narrow band rather than uniformly distributed, the concentration distribution of the microcomponent during elution as a function of time and distance can be calculated. The elution dynamics used in considering the band elution case were those of partition chromatography. The elution curve is extremely dependent on the diffusional properties of the system. At equilibrium the "limiting" equations (Equation (15), (16), and (17)) are followed. Thus the volume of elutriant necessary for the elution of the peak in a band distribution equals that necessary for the elution of an uniformly distributed case (31, 34, 38). However, for fractional elution of a component, the band distribution located at the top of the resin provides an overestimation of the amount of elutriant required.

5.4 Column Dimensions

Theoretical studies made for the elution process under equilibrium conditions and linear isotherms consider only the total volume of the resin and not column dimensions. Experiments (34) were run to determine the importance of column dimensions. Under equilibrium conditions, it was found that elution is relatively insensitive to column dimensions. A three-fold variation in column length produced slight (maximum 15%) differences between the calculated and experimental elution volumes. It was felt

by the experimenters (34) that these differences were caused by diffusional effects.

5.5 Non-Equilibrium Elution

The regeneration of ion exchange columns under non-equilibrium conditions is a more complicated situation and a theory explaining the kinetics has not been adequately developed. However, corrections at least to a first-order approximation, can be made from the results of front formation theory (16). These corrections indicate how much additional elutant is needed for the non-equilibrium elution.

Rachinski and Rustamov (36) divided the regeneration process into two stages. First, in an infinitely thin layer at the column inlet, a non-equilibrium ion exchange occurs until the resin is primarily in the eluted form. Second, the entire column is regenerated by the equilibrium process of spreading this thin layer along the column. The volume of elutriant required can be expressed as the sum of two volumes

$$V_R = V_1 + V_2 \qquad (18)$$

where

V_1 = volume of elutriant used in stage 1

V_2 = volume of elutriant used in stage 2 and is calculated by Equation (15), (16), or (17).

V_1 is calculated for an exhausted bed by

$$V_1 = \frac{u}{\beta} \frac{Q}{h} \int_0^{\theta} \frac{d\theta}{1-f(\theta)} \tag{19}$$

or for a partially exhausted bed by

$$V_1 = \frac{u}{\beta} \frac{Q}{h} \int_{\theta_1}^{\theta_2} \frac{d\theta}{1-f(\theta)} \tag{20}$$

u is the average linear velocity in the column

h is the ratio of the solution and resin normality per unit column length

n_0 is the solution normality in meguivalents per unit column length

N_0 is the resin capacity in meguivalents per unit column length

θ is the relative concentration of an ion in the resin, N/N_0

Q is the cross sectional area for solution transport in the column

β is the effective rate constant for the absorption of the exchanging ions

ϕ is the relative concentration in the solution phase n/n_0

$f(\theta)$ is the θ dependence of the dimensionless sorption isotherm

The sorption isotherm, Equation (14) can be dimensionlessly represented by

$$\frac{1-\theta}{\theta} = B\frac{1-\phi'}{(\phi')^2} \tag{21}$$

ϕ' is the relative equilibrium concentration of the solution in contact with a resin of composition θ

$$B = k_{1,2}^{Z_1} h^{1-\lambda} \tag{22}$$

λ is the ratio of the valences of the eluted ion, Z_1, to the eluting ion, Z_2.

In order to find the functions $f(\theta)$ and θ for Equation (19) or (20) from Equation (21), a parameter "S" is introduced for mathematical convenience

$$S = \theta/\phi' \tag{23}$$

from which

$$f(\theta) = \phi' = \frac{1-BS^{\lambda}}{S(1-BS^{\lambda-1})} \tag{24}$$

$$\theta = \frac{1-BS^{\lambda}}{1-BS^{\lambda-1}} \tag{25}$$

Using the relationship for $f(\theta)$ and θ in Equation (20) yields

$$V_1 = \frac{uQ}{\beta h} \int_{S_1}^{S_2} \frac{B[(\lambda-1)(1-BS^{\lambda})S^{\lambda-1} - \lambda(1-BS^{\lambda-1})S^{\lambda}]dS}{(1-BS^{\lambda-1})(S-1)} \qquad (26)$$

Integration of this equation for the iron-thorium case, $\lambda = 4/3$, gives

$$V_1 = \frac{uQB}{\beta h 3} \left\{ S/B - S^{4/3}/4 + 3(1-BS^{1/3})^2/(2B^4) + 3 \ln (1-BS^{1/3})/B^3 - 3/2 \ln \frac{(S^{1/3}-1)^2}{(S^{2/3}+S^{1/3}+1)} - 6(1-BS^{1/3})/B^4 - 3\sqrt{3} \tan^{-1}[(-2S^{1/3}+1)/\sqrt{3}] \right\} \Bigg|_{S_1}^{S_2} \qquad (27)$$

Inspection of the terms in Equation (27) provides information concerning the parameters of loading, and column dimenions. For the iron-thorium system $B >> 1$ (thorium is preferred by the resin phase i.e., the isotherm for iron equilibrium is concave) and for thorium trace loaded, S can be approximated by Q_{Fe} . This can be shown by considering the fact that if thorium is preferred by the

resin then the equivalent fraction of iron in the solution phase must be larger than that in the resin phase at equilibrium. Thus if θ_{Fe} is close to 1 (thorium trace loaded) then ϕ'_{Fe} must be even closer ($B >> 1$) and S_{Fe} is approximately θ_{Fe} (see Equation (21)). Inside the { } the most significant term is $\ln\left(\frac{S_1^{1/3}-1}{S_2^{1/3}-1}\right)$. By insertion of different values of iron loading, it was readily apparent that, for different trace loadings of thorium, V_1 would be approximately constant if the fraction of thorium removed remained the same. This occurs over a range of initial throium (or iron) loadings. Table 5 illustrates this fact for several thorium loadings, .5 - 5.%, and a 90% elution of thorium where S_1 ($\theta_{Fe} = 1-\theta_{Th}$) is the initial fraction of iron on the iron-thorium loaded resin and S_2 is the fraction of iron after removal of 90% of the thorium (θ_{Fe_2}). Inspection of the term outside the { } indicates that if u is a constant, it would be preferable to have a small diameter column (small Q). This would increase the length of the column and hence the contact time allowing a closer approach to equilibrium. Although, from Equation (27), it appears that the excess volume is linear in flow rate, β is velocity dependent.

$$\frac{u}{\beta} = \frac{u}{\beta^*} + \frac{u}{\beta^{**}} + \frac{D^*}{u} \qquad (28)$$

Table 5

Variation of $\ln((S_1^{1/3}-1)/(S_2^{1/3}-1))$ For Different Loadings of Thorium and 90% Elution

$\theta_{Th}=1-\theta_{Fe}$	$S_1 (\approx \theta_{Fe_1})$	$S_2 (\approx \theta_{Fe_2})$	$\ln\left(\frac{S_1^{1/3}-1}{S_2^{1/3}-1}\right)$
.05	.95	.995	2.318
.04	.96	.996	2.315
.03	.97	.997	2.312
.02	.98	.998	2.309
.01	.99	.999	2.306
.005	.995	.9995	2.304

β^* is the rate constant for the diffusion from the resin to the solution

β^{**} is the rate constant for diffusion inside the exchanger, and

D^* is the effective constant for longitudinal diffusional transfers (16)

Inspection of the function dependency of the terms in Equation (28) indicates that it is only at very low flow rates (or velocities) that β is strongly velocity dependent. Hence until very low flow rates are encountered, the excess solution can be considered linear in flow rate.

The importance of trace ion distribution (either band or uniform distribution) in the column is harder to define for the non-equilibrium case. Here both distributions have the same dependence on flow velocity but the excess solution for the band distribution is larger for the same fractional elution of a given loading, Equation (27). Thus, as in the equilibrium case, the band distribution yields an overestimation of the amount of elutriant needed for the elution.

CHAPTER VI

PROCESS AND CALCULATIONAL EXAMPLE

The elution step studied is only part of a process to be used in decontaminating radioactive ion exchange resins. An example of how this process works is given below. Calculations of selected ions present on a resin after one year of reactor service were obtained from Stone and Webster (39). From this listing, the radioactive ions which had half-lives longer than 1 month were selected for use in this example.

The ions selected, their primary valence, and their activity are listed in Table 6 (39).

Iodine is present in much greater quantities than listed in Table 6 when the resin is removed from the reactor coolant system; however, the isotopes involved have very short half-lives (from seconds to a few days) and times spent in storage would bring the activity down to a low level without any processing.

Although niobium and technetium have higher valences, they will be classed in the cesium rather than the thorium group since both ions have distribution coefficients much less than 1($D << 1$) in less than .2M HCL (18). Hence these ions will be eluted extremely rapidly (prior to cesium).

For calculational ease, all the radioactivity will

Table 6

Radioactive Ions Used In Elution Example

Ion	Valence	Activity (Curies)
I-129	-1	$4.1 \cdot 10^{-3}$
Cs-134	+1	$2.3 \cdot 10^{+4}$
Cs-137	+1	$6.1 \cdot 10^{5}$
Co-58	+2	$3.0 \cdot 10^{2}$
Co-60	+2	$1.4 \cdot 10^{2}$
Fe-59	+2	$1.9 \cdot 10^{-1}$
Sr-89	+2	$5.5 \cdot 10^{1}$
Sr-90	+2	1.0
Mn-54	+2	1.8
Cr-51	+3	$3.6 \cdot 10^{1}$
Y-91	+3	$1.0 \cdot 10^{3}$
Nb-95	+5	$6.3 \cdot 10^{-1}$
Tc-99	+7	$9.6 \cdot 10^{2}$
	Total	$635.5 \cdot 10^{3}$

be assumed to be in 2 ft.^{3} of resin (1 ft.^{3} cation and 1 ft.^{3} anion resin).

Using experimental data presented in this report, the elution step is described. Operating conditions which would improve the effectiveness of the elution by decreasing the amount of salt required are written parenthetically after the values used in the example. Experimental data regarding the effectiveness of the elution under the recommended operating conditions was not obtained. Hence the recommended operating conditions could not be used in the calculational example.

In the decontamination process, the resins are removed from the reactor and placed in storage to allow the short term activity to decay. This storage time can vary but should probably be in the vicinity of 1 week to 1 month. Longer times could be used to allow for more decay however.

The resin is then separated into its anion and cation components. This is a standard procedure and is accomplished by rapidly flowing water up through the resin and allowing the resins to separate due to density differences. This also provides a washing of the resin to remove any crud or particulate matter accumulated during reactor operation. This water is evaporated and the radioactive residue collected for desposal.

In the loading chosen to illustrate the process, most of the activity on the anion resin is short-term

and will rapidly decay away. The remaining activity is present in such small quantities (millicuries in the example) that it is probably preferable to ship the anion resin as is rather than process it. Iodine-131 has an eight day half-life (all the higher isotopes have half-lives less than one day) and the storage time to allow for decay will be controlled by the activity of this isotope if processing is decided against. For the example, the processing step for the anion cesium is omitted. If there is a desire to process the anion resin, the same techniques as used in the cation elution would apply.

After the resins are separated, the cation resin is placed in a long column (a length to diameter ratio of at least 6). This is to increase the contact time between the elutriant and the resin. A dilute ferric chloride solution, .13N, at ambient temperature is run through the column at a flow rate of 2 gpm/ft^2 ($\frac{1}{8}$ gpm/ft^2).

When 25.9 ft^3 solution/ft^3 resin (see Section 4.4) is passed through the column, approximately all of the cesium group (Cs-134, Cs-137, Nb-95, and Tc-99) will have been eluted from the resin. From Figure 16, at least 25% of the barium group (Co-58, Co-60, Sr-89, Sr-90, Mn-54, and Fe-59) has been eluted. From Figure 13 at least 10% of the scandium group has been eluted (Y-91 and Cr-51). These ions have smaller distribution coefficients than their respective test ion (cesium, barium, scandium) and hence

are eluted to a greater extent than their representative ions. However the degree of increase is not known. If the elution were to be discontinued at this point, better than 99% of the radioactivity would have been removed. This value of 99% removal is for the specified conditions, situations can occur like the Connecticut Yankee cobalt-58 problem where the major contaminant is cobalt-58, a barium group ion. In this case only a minimum of 25% of the radioactivity would have been eluted.

The effluent from the column is placed continuously into an evaporator and residue collected. The ion residual volume would be 2.6% of the cation resin volume at the point of process.

Continuing the elution with ferric chloride to elute the barium group, an additional 46.2 ft^3 solution/ft^3 cation resin elutes at least 96% of the barium group and at least 76% of the scandium group (Section 4.3 and Figure 13 respectively). The total ion residue volume is 14.4% of the cation resin volume.

At this point the ferric chloride solution is not as effective an eluting agent as a concentrated ferric sulfate solution, 0.94N(1.N), and the elutriant should be switched. The new eluant has a flow rate of 1/4 gpm/ft^2(.01 gpm/ft^2). From Figure 13, the difference in iron for 24% scandium remaining on the column and 1% is 21.6 grams. Converting this into solution volume yields 4.2 ft^3 solution/ft^3 resin

$$\left(\frac{21.6}{.3}\right)\left(\frac{3}{55.5}\right)\left(\frac{1}{.94}\right) = 4.2\ \frac{\text{vol soln}}{\text{vol resin}} \qquad (28)$$

21.6 - mass of iron required, gms
$\frac{55.5}{3}$ - equivalent mass of iron, gms/equivalent
.3 - column volume, l
.94 - normality of solution, equivalent/l

After 4.2 ft^3 solution per cubic foot resin, better than 99% of the scandium group and all of the barium group except for the alkaline earth fraction which formed a sulfate precipitate (at most 4% of initial barium group activity) is eluted. If the elution is to be terminated at this point, water should follow the ferric sulfate solution after 4.2 cubic feet of elutriant per cubic foot of resin has entered the column. This is done to avoid excess residual salt volume from any elutriant in the resin's void volume after the required amount of elutriant has passed through the resin.

Evaporation of the solution increases the total ion residue by 10.5% to a total of 24.9% of the <u>cation</u> resin volume.

$$\left(\frac{21.6}{111}\right)\left(\frac{4.35.10^2}{2.7.10^3}\right)\left(\frac{1}{.3}\right) = .105 \qquad (29)$$

111 -formula weight of iron in $Fe_2(SO_4)_3$
435 -formula weight of $Fe_2(SO_4)_3 .2H_2O$
$2.7.10^3$-density $Fe_2(SO_4)_3 .2H_2O$, 9M/l
.3 -volume of experimental column, cc

At this point the radioactivity should have been substantially removed from the resin. The effluent is evaporated and residue prepared for disposal. The resin is also made ready for disposal.

Table 7 is a summary of the elution data given in the process example.

The elution is not limited to the set of conditions outlined in the example. If the composition of ions on the resin were different from those of the example and a heavy preponderance of the activity were with higher valence ions, the eluting solution should be changed from the ferric chloride to the ferric sulfate solution earlier in the process. This is to take advantage of the complexing properties of the sulfate, which aid in the elution of heavy metal ions. Thus, at least a qualitative knowledge of what ions are on the resin should be obtained in order to more effectively apply the elution techniques developed in this report.

Table 7

Example Process Data

Salt	Co N	W gpm/ft^2	Vol. Solution / Vol. Resin	fract. of resin vol. in salt residue (total)	% of activity/ group removed	Group
$FeCl_3$	0.13	2(1/8)	25.9	.026	100	Cesium
					25	Barium
					10	Scandium
$FeCl_3$	0.13	2(1/8)	46.2	.144	100	Cesium
					96	Barium
					76	Scandium
$Fe_2(SO_4)_3$	0.94	1/4(.01)	4.2	.249	100	Cesium
					96	Barium
					99	Scandium

CHAPTER VII

CONCLUSIONS AND RECOMMENDATIONS

Elution by neutral salts is a technically feasible process for the substantial concentration of the radioactivity initially on the exchangers when removed from the reactor.

Table 8 provides a summary of the best operational conditions based upon evaluation of the experimental data (from Section 4).

A preliminary economic analysis was not made for the proposed elution process due primarily to insufficient economic information in both the present and proposed disposal process.

The amount of salt needed for the elution could be reduced from the level determined experimentally. This would be accomplished by using better operating conditions than those experimentally investigated. The major recommendation in this area would be to use slow flow rates: 1/8 gpm/ft^2 for elution with the dilute ferric chloride solution and 1/2 gpm/ft^2 with the sodium sulfate solution (anion exchange) and .01 gpm/ft^2 for the concentrated ferric solution. It is also recommended that ambient rather than elevated temperatures be used for the elution step.

Due to the importance of flow rate in determining

Ion	Salt	Co (N)	W gpm/ft^2	T	fraction ion eluted	fraction of resin vol. in dried residual salt	Vol. Sol'n / Vol. Resin
Cs^{+1}	$FeCl_3$	.13	2	ambient	1.00	.026	25.9
Ba^{+2}	$FeCl_3$	.13	2	ambient	.96	.144	76.1
Sc^{+3}	$Fe_2(SO_4)_3$	.94	1/4	ambient	.99	.153	8.2
Th^{+4}	$Fe_2(SO_4)_3$	.94	1/4	ambient	.90	.256	12.4
I^{-1}	Na_2SO_4	.18	2	ambient	1.00	.164	113

Table 8

Best Experimental Elution Data

of the excess volume of elutriant required, the first area for any further research would be to determine better the effect of very low flow rates. Part of this information could be obtained from field experience with the process. Another important area would be the testing of more effective eluting agents, specifically for the anion resin.

Effects of column length and regenerant concentration are areas for further investigation. However, this information could in most part be obtained from operational experience and evaluation of engineering data.

APPENDIX A

ELUTION CONDITIONS AND TYPICAL RUNS

Table 9

Summary of Elution Conditions

Run #	Eluting Agent	Concentration (N)	Flow Rate (gpm/ft^2)	Temp.	pH	Loading %	Fig. No.
			THORIUM				
1	NaCl	0.88	1/2	ambient	6.0	1.0	--
2	NaCl	0.88	1/2	ambient	7.0	1.0	--
3	NaCl	0.88	1/2	ambient	3.0	1.0	--
4	NaCl	1.84	1/2	ambient	3.0	1.0	--
5	NaCl	1.84	1/2	ambient	3.1	100.0	11
6	$Fe_2(SO_4)_3$	0.94	1	ambient	1.5	1.0	2,4,6,9
7	$Fe_2(SO_4)_3$	0.94	2	ambient	1.5	1.0	4,6,9
8	$Fe_2(SO_4)_3$	0.94	1/2	ambient	1.5	1.0	3,4,6,7,9
9	$Fe_2(SO_4)_3$	0.431	1/2	ambient	1.5	1.0	3,7,9
10	$Fe_2(SO_4)_3$	1.97	1/2	ambient	1.5	1.0	3,5,7,9
11	$Fe_2(SO_4)_3$	0.94	1/4	ambient	1.5	1.0	4,5,6,9,10
12	$Fe_2(SO_4)_3$	0.94	1/4	ambient	1.5	1.0	10

Table 9 (Cont.)

Run #	Eluting Agent	Concentration (N)	Flow Rate (gpm/ft^2)	Temp.	pH	Loading %	Fig. No.
13	$Fe_2(SO_4)_3$	0.94	1/4	75°C	1.5	1.0	5,8
14	$Fe_2(SO_4)_3$	1.97	1/2	75°C	1.5	1.0	5,8
			CESIUM				
15	$Fe_2(SO_4)_3$	0.93	1/4	ambient	1.5	1.0	18
17	$Fe_2(SO_4)_3$	0.36	1	ambient	1.5	1.0	18
18	$Fe_2(SO_4)_3$	0.154	2	ambient	1.5	1.0	17,18
19	$FeCl_3$	0.13	2	ambient	1.5	1.0	17.18
			BARIUM				
16	$Fe_2(SO_4)_3$	0.94	1/4	ambient barium precipitated	1.5	1.0	--
17	$Fe_2(SO_4)_3$	0.36	1	ambient barium precipitated	1.5	1.0	--
18	$Fe_2(SO_4)_3$	0.154	2	ambient barium precipitated	1.5	1.0	--
19	$FeCl_3$	0.13	2	ambient	1.5	1.0	16

Table 9 (Cont.)

Run #	Eluting Agent	Concentration (N)	Flow Rate (gpm/ft^2)	Temp.	pH	Loading %	Fig. No.
			SCANDIUM				
16	$Fe_2(SO_4)_3$	0.94	1/4	ambient	1.5	1.0	12,13,14
17	$Fe_2(SO_4)_3$	0.36	1	ambient	1.5	1.0	13,14
18	$Fe_2(SO_4)_3$	0.154	2	ambient	1.5	1.0	13,14
19	$FeCl_3$	0.13	2	ambient	1.5	1.0	13,14,15
			IODIDE				
20	Na_2SO_4	0.18	2	ambient	1.5	1.5	19

Table 10

Thorium Elution Using $Fe_2(SO_4)_3$ as the Eluting Agent at

Co = 0.94N, W = 1/4 gpm/ft^2, Ambient Temperature, pH = 1.5, Run 11

Sample	Sample Vol. ml.	Thorium in Sample (mg.)	Thorium total Thorium in effluent (mg.)	Ferric Iron Normality of sample (N)	Total Iron in Effluent (gms)
1	250	9.68	9.68	0.0006	0.003
2	250	79.24	88.9	0.107	0.5
3	250	43.75	132.7	0.251	1.67
4	250	27.37	160.0	0.417	3.6
5	250	24.61	184.7	0.555	6.2
6	250	21.74	206.4	0.738	9.6
7	250	17.97	224.4	0.811	13.4
8	500	27.20	251.6	0.831	21.3
9	250	10.43	262.0	0.895	25.5
10	250	9.71	271.7	0.925	29.8
11	250	9.28	281.0	0.936	34.2
12	250	8.87	289.9	0.945	38.6
13	250	7.36	297.2	0.94	42.9

$$\frac{\text{Volume of dried salt}}{\text{Volume of Cation resin}} = 0.205$$

Fraction of Thorium Eluted = 0.854

Table 11

Cesium Elution Using $FeCl_3$ as the Eluting Agent at

Co = 0.13N, W = 2 gpm/ft^2, Ambient Temperature, pH = 1.5, Run 19

Sample	Sample Vol. ml.	Cesium		Ferric Iron	
		Fraction of Cesium Load. per Sample	Total Fraction of Cesium Eluted	Normality of Sample (N)	Total Iron in effluent (gms.)
1	2000	0	0	0	0
2	2000	0	0	0	0
3	1000	0.638	0.638	0.037	0.69
4	1000	0.309	0.947	0.119	2.9
5	1000	0.050	0.997	0.127	5.3
6	1000	0.003	1.000	0.129	7.7
7	1000	0	0	0.129	10.1
8	1000	0	0	0.128	12.4

$$\frac{\text{Volume of dried salt}}{\text{Volume of cation resin}} = 0.026$$

Fraction of Cesium Eluted = 1.00

Table 12

Iodide Elution Using Na_2SO_4 as the Eluting Agent at
Co = 0.18N, W = 2gpm/ft^2, Abient Temperature, pH = 1.5, Run 20

Sample	Sample Vol. ml.	Iodide in Sample mg	Total Iodide in Effluent mg	Sulfate Normality of Sample (N)	Total Sulfate in Effluent (gms.)
1	2000	0	0	0	0
2	1000	0	0	0	0
3	1000	0	0	0.155	7.4
4	1000	0	0	0.162	15.2
5	1000	0	0	0.174	23.5
6	1000	0	0	0.175	32.0
7	1000	0	0	0.177	40.4
8	1000	0	0	0.177	48.9
9	1000	0	0	0.177	57.4
10	1000	41	41	0.177	65.9
11	1000	457	498	0.177	74.4
12	1000	242	740	0.177	82.8
13	1000	20	760	0.177	91.3
14	1000	0	760	0.177	99.8

$$\frac{\text{Volume of dried salt}}{\text{Volume of anion resin}} = 0.164$$

Fraction of Iodide Eluted = 1.00

APPENDIX B

ANALYTICAL TECHNIQUES

B.1 Colorimetric Analysis

Calorimetric techniques were used in the analysis of thorium and iron. A Beckman spectrophotometer, model DK-1A, was used for the analysis.

B.1.1 Statistical Methods

Calibration charts were made for thorium and iron. Colorimetric reagents were used in which the other components of the system did not interfer. A calibration was performed for each system; the standard curve was obtained by regression analysis and the variance for different concentrations was obtained.

The equations required for the derivation of the standard curve were found in Calder (40) and presented below. For this derivation n is the total number of observations made for c different concentrations where y is the predicted absorbance for concentration x and z is the average observed absorbance at that concentration.

The standard curve passes through the point $(\bar{x},\bar{y})$ with its slope given by

$$m = \frac{\sum xy - \sum x \sum z/n}{\sum(x^2) - (\sum x)^2/n} \qquad (30)$$

and the regression equation is

$$y - \bar{z} = m(x-\bar{x}) \qquad (31)$$

The variance, S_x^2, of a value of x determined from the observed reading z is given by

$$S_x^2 = \left[S_4/(c-2)\right] \; /m^2 \left\{ 1 + 1/c + (z-\bar{z})^2 / \left[m^2 \Sigma (x-\bar{x})^2\right] \right\} \qquad (32)$$

$$S_y = \frac{n}{c}(\Sigma z^2) - (\Sigma y)^2/n - \frac{n}{c}\left[\frac{(\Sigma xz - \Sigma x \Sigma z/c)^2}{\Sigma x^2 - (\Sigma x)^2/c}\right] \qquad (33)$$

From these formulae, limits of error may be predicted.

B.1.2 Iron Analysis

Griffing and Mellon (41) studied the effects of reagent concentration, pH, order of addition of reagents, times of reaction, iron concentration, and diverse ions on the determination of iron using nitroso-R-salt. Sodium, sulfate, and chloride do not interfer; thorium in quantities less than 100 ppm did not interfer.

A stock iron solution .1000M was prepared by dissolving oven-baked reagent ferric oxide, Fe_2O_3, in hydrochloric acid. A solution containing .0100M was obtained by dilution with deionized water. The reagent solution contained 0.5% nitroso-R-salt and 30% reagent acetone. A 10% solution of hydroxylamine hydrochloride was used as a

reducing agent since the colored complex formed was with the ferrous ion. Adjusting the pH was accomplished using a 4M sodium acetate solution and a 1.5M ammonia solution.

Experimentally the following conditions were observed. To a 50 ml. volumetric flask, a sample containing 1-90 ug of iron was added; then 3 ml of the reducing agent and 3ml of the reagent were added in this order; the pH was adjusted to 4.6±0.1 (allowable range 4.6±0.5); dilution to 50 ml; and finally a development time of 3 hours was allowed. The transmission was measured at 665 mu against a water blank.

From the calibration curve, Figure 20, the equation relating ug Fe to the absorbance are

Range 1-30 ug

$$Fe(ug) = 66.388 \text{ (absorbance)} - 2.3723 \qquad (34)$$

Range 30-90 ug

$$Fe(ug) = 68.913 \text{ (absorbance)} - 2.7990 \qquad (35)$$

Although one straight line could have been drawn through the data, a better fit was obtained if 2 were used.

The error of prediction was less than 2%.

In determining the iron content of an unknown, three separate determinations were made. Multiple determinations were made primarily as a check against inadequate mixing or sample preparation. Three samples were prepared to avoid a long delay due to development time if two samples did not

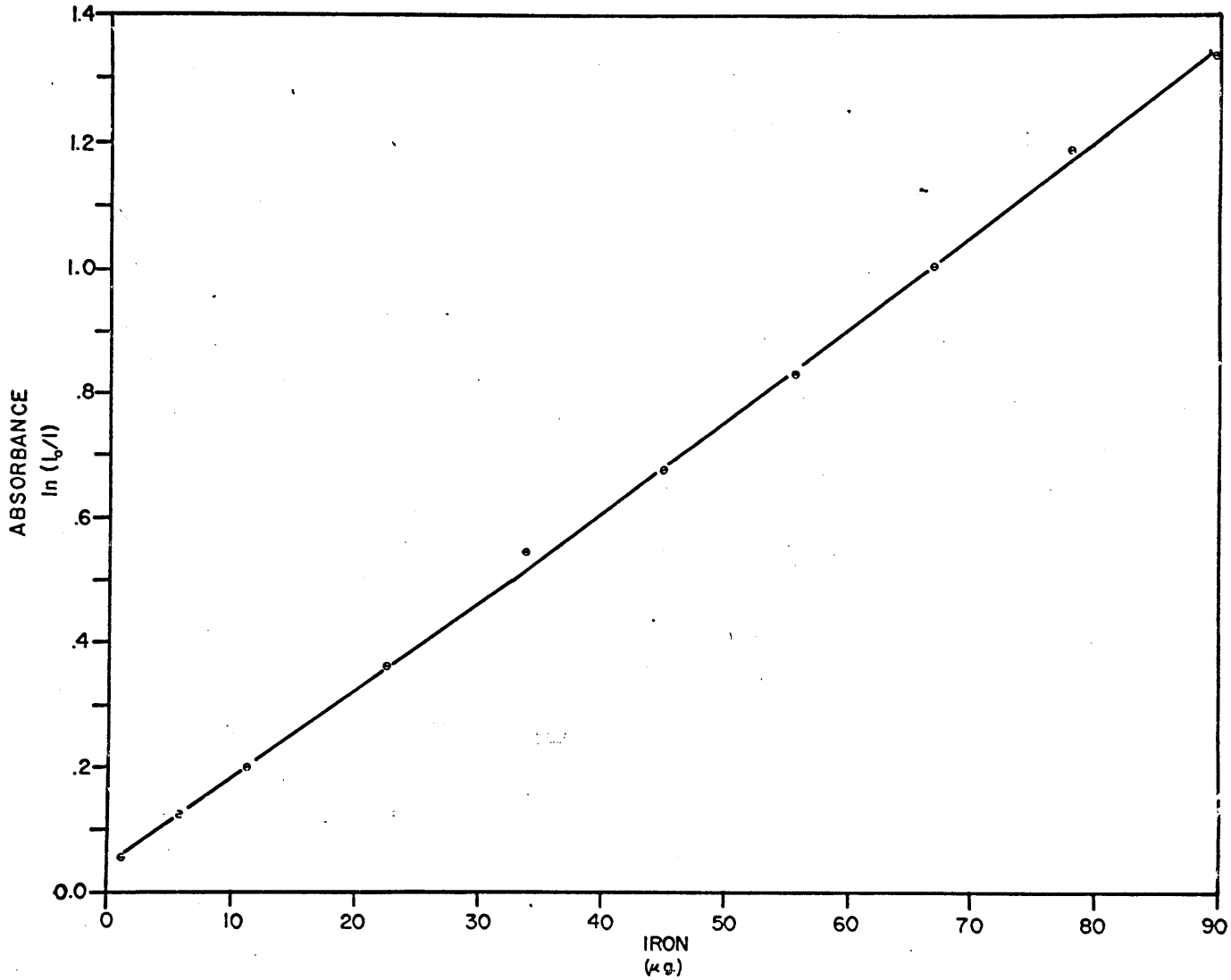

Figure 20 Iron calibration curve using Nitroso-R as colorimetric agent

closely match. This reasoning carried over to the thorium analysis although sample preparation was easier and less time was required.

B.1.3 Thorium Analysis

Two colorimetric techniques were used in the determination of thorium. Carminic acid was used for analysis of thorium in the presence of sodium and arsenazo III for thorium in iron.

A thorium standard was made by dissolving reagent anhydrous thorium chloride in deionized water, solutions of different concentrations were made by dilution of the standard.

Procedure I

Snell, Snell and Snell (42) described a colorimetric technique for the determination of thorium using carminic acid. The complex formed is stable with respect to time although close control of the pH is necessary as the thorium complex is also an indicator. Sodium does not interfer with the stability of the thorium complex, however, iron forms an identical complex and so interfers seriously.

The reagent solution is a .02% solution of carminic acid heavily buffered to a pH of 4.2 by the acetic acid-sodium acetate system.

The experimental procedure is straightforward, mix 1 ml of sample containing 25-200 ug of thorium with 9 ml of

reagent, dilute to 10 ml, and read at 575 mu against a water standard.

The calibration curve is found in Figure 21. The equation for this line is

$$Th(ug) = 45.57\ (absorbance) + 2.01 \qquad (36)$$

The error is ~2%.

Although sodium did not interfer in the determination of thorium by forming complexes with the carminic acid, the concentration of thorium in the samples was so low that partial evaporation of a larger sample was sometimes necessary in order to obtain a measureable quantity of thorium. The large amount of sodium chloride present affected the physical properties of the solution and hence its absorbance per unit path length. This introduced an error of unknown quantity but of which tended to increase absorbance and hence inflate the value of thorium present.

Procedure II

Savvin (43) reported on the use of arsenazo III for the determination of thorium. Iron is masked by ascorbic acid and the choice of pH.

In the determination of thorium, a sample containing 1 to 30 ug of thorium was placed in a 25 ml volumetric flask, 1 ml of 10% ascorbic acid solution was added, 1 ml of .05% arsenazo III solution, 10 ml of water, add 6 ml of hydrochloric acid (sp gr 1.19); dilute to volume, and

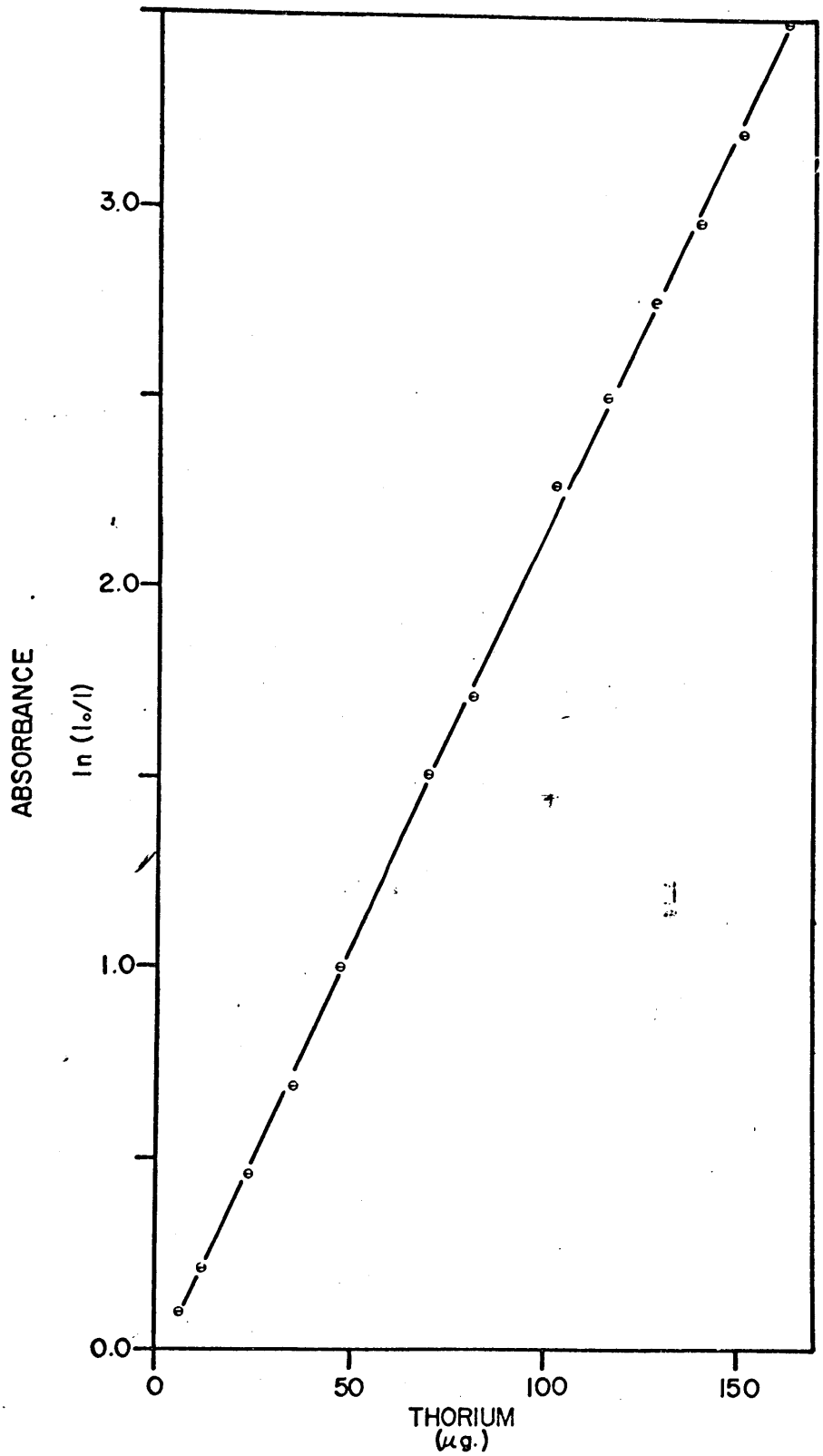

Figure 21 Thorium calibration curve using Carminic Acid as colorimetric agent

read the absorbance at 665 mu against a reagent blank. It was important to add water prior to the acid otherwise a partial decomposition of the reagent took place.

A calibration curve, Figure 22, was prepared. The equation for the regression line is

$$\text{Th (ug)} = 32.583\ (\text{absorbance}) + 0.10428 \qquad (37)$$

Error ~1%.

In practice of iron is present the color tends to fade after one hour, measurements were made within 10 minutes of mixing. If iron is not present, the color complex is stable for times up to 2 days depending on conditions of preparation.

In procedure I each determination was made twice, while in procedure II, 3 times.

B.2 Radioactive Tracer Analysis

Cesium, barium, and scandium were analyzed by a method of radiochemical analysis in which the amount of an element in a given sample is directly proportional to its gamma-ray absorption peak.

Covell (44) describes a statistical method which performs a numerical analysis of the values making up the absorption peak curve and allows a direct reduction of the data. This technique is especially applicable where the radiations from several nuclides are involved; it primarily consists of taking the channel in an absorption

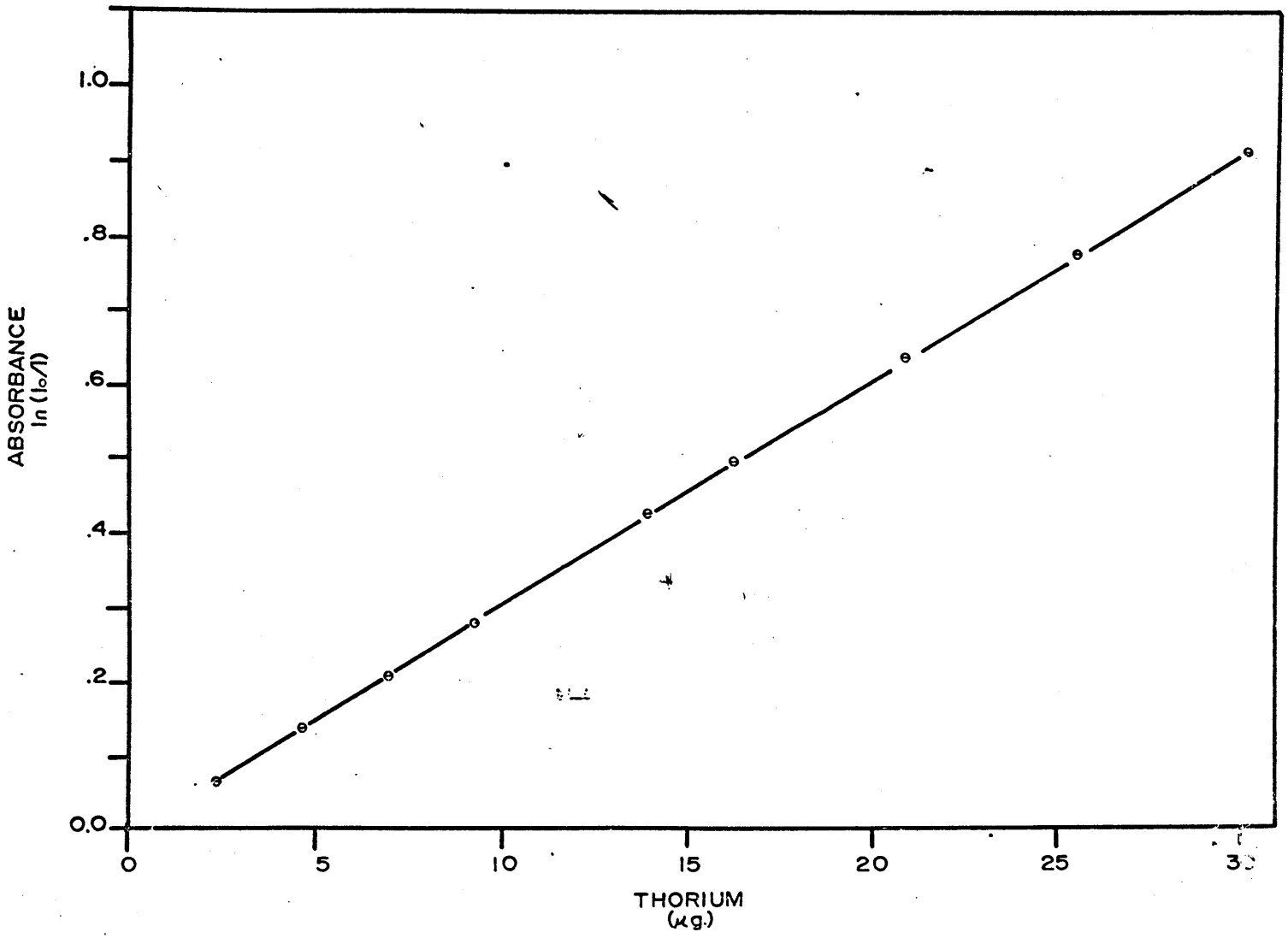

Figure 22 Thorium calibration curve using Arsenazo III as colorimetric agent

peak with the greatest number of counts, a_o, and n channels on either side of a_o and reducing this data to a form which yields the desired information. These channels are designated a_i or b_i $(i=1,n)$ depending on whether they are on the low amplitude side of a_o or on the high side.

The total number of counts in these 2n+1 channels is taken and represented graphically as an area. This area can be divided by a line connecting the ordinate values of a_n and b_n with the area above the line represented by

$$N = a_o + \sum_{i=1}^{n} a_i + \sum_{i=1}^{n} b_i - (n+1/2)(a_n + b_n) \quad (38)$$

This area, N, should bear a constant relationship to the total area contained in the peak or more precisely to the activity producing that photopeak. If a Poisson distribution is assumed for each of the 2n+1 terms, the estimated variance is

$$\sigma(N) = \sqrt{N + (n-1/2)(n+1/2)(a_n + b_n)} \quad (39)$$

The variation involved in taking sample volumes was less than 1 percent, the same being true for the comparison standard.

Experimentally, the procedure for this method of analysis was straightforward. Two milliliters of each collected effluent volume were poured into a polyethylene vial. This vial was placed in a NaI well detector and

the number of counts from a specific radioisotope in a given time interval was determined. Comparison of the reduced data thus obtained, with that of a standard similiarly prepared which contained $(1.00 \pm .01) .10^3$ of the tracer input to the column, gave a measure of the total amount of test ion that was eluted per unit effluent volume.

The isotopes used were barium-133, cesium-137, and scandium-46.

Cesium involved a slightly altered data reduction procedure. Although unintentional, the activity of cesium-137 for the 1% column loading was lower than that of either barium or scandium. The cesium photopeak also overlapped the beginning of the Compton edge for scandium-46, presenting an additional difficulty in determining the presence of small quantities of cesium. This overlap necessitated that the scandium photopeak be "stripped out" out the spectrum prior to analysis.

B.3 Titrimetric Analysis

This is the technique used in the analysis of sulfate and iodide. In this technique, the volume of a known reagent needed to bring a reaction to completion is determined.

B.3.1 Iodide

The determination of iodide by iodimetry is one of the basic methods used in quantitative analytical chemistry (45).

The iodide present in a sample is oxidized to iodine which is reacted with sodium thiosulfate. The volume of the sodium thiosulfate solution used is a measure of how much iodide was present in the sample initially.

The procedure for this analytical method is as follows: 100 milliliters of sample was added to a 500 ml glass-stoppered flask, 1 gram of urea, 2 ml of 2M sodium nitrite solution, and 10 ml of 4N phosphoric acid were also added. The flask was stoppered and allowed to stand with frequent shaking for 10 minutes.

In acid solution, the following reaction takes place quantitatively.

$$4H^+ + 2NO_2^- + 2I^- \rightarrow 2NO + I_2 + 2H_2O \qquad (40)$$

The excess nitrite and nitric oxide are removed by the urea.

$$\begin{aligned} 2NO_2^- + CO(NH_2)_2 + 2H^+ &\rightarrow 2N_2 + CO_2 + 2H_2O \\ 6NO + CO(NH_2)_2 &\rightarrow 5N_2 + 2CO_2 + 2H_2O \end{aligned} \qquad (41)$$

Since these reactions are slower than that of the nitrite and the iodide, it is possible to add the urea at the start. Urea was again added after 10 minutes to insure the complete removal of nitrite and nitric oxide. Chloride and sulfate do not interfer. Interference from the ferric ion which reacts with the iodide

$$2Fe^{+3} + 2I^- \rightleftarrows 2Fe^{+2} + I_2$$

is prevented by the addition of phosphoric acid.

After a suitable amount of time, 2 gms of potassium iodide to dissolve the iodine as KI_3 plus 20 ml at carbon tetrachloride were added to the solution. This solution was then titrated with .114N sodium thiosulfate (standardized against copper).

$$2Na_2 S_2 O_3 + I_2 \rightarrow 2NaI + Na_2 S_4 O_6 \qquad (42)$$

An iodide standard (20 mg/ml) was prepared and a calibration curve, Figure 23, was made for the purpose of determining the error (<1%) in the analysis.

$$I\ (mg) = 14.2207\ (ml) + .1672 \qquad (43)$$

B.3.2 Sulfate

Eriochrome Black T was used as the metallochrome indicator in the well-known titration of sulfate with barium chloride. The technique used (46) was intended to minimize the interterence of iron present in the system. When iron was absent, the transition of the indicator from a blue coloration to a red-purple was more clearly defined.

The procedure is straightforward. A sample containing 2-20 mg of sulfate was poured into a beaker, the solution was made slightly acidic (pH 2-3) using acetic acid; 5 ml of .2M DCyTA (1,2 diaminocyclohexanetetraacetic acid) was added to mask any iron present and the solution boiled.

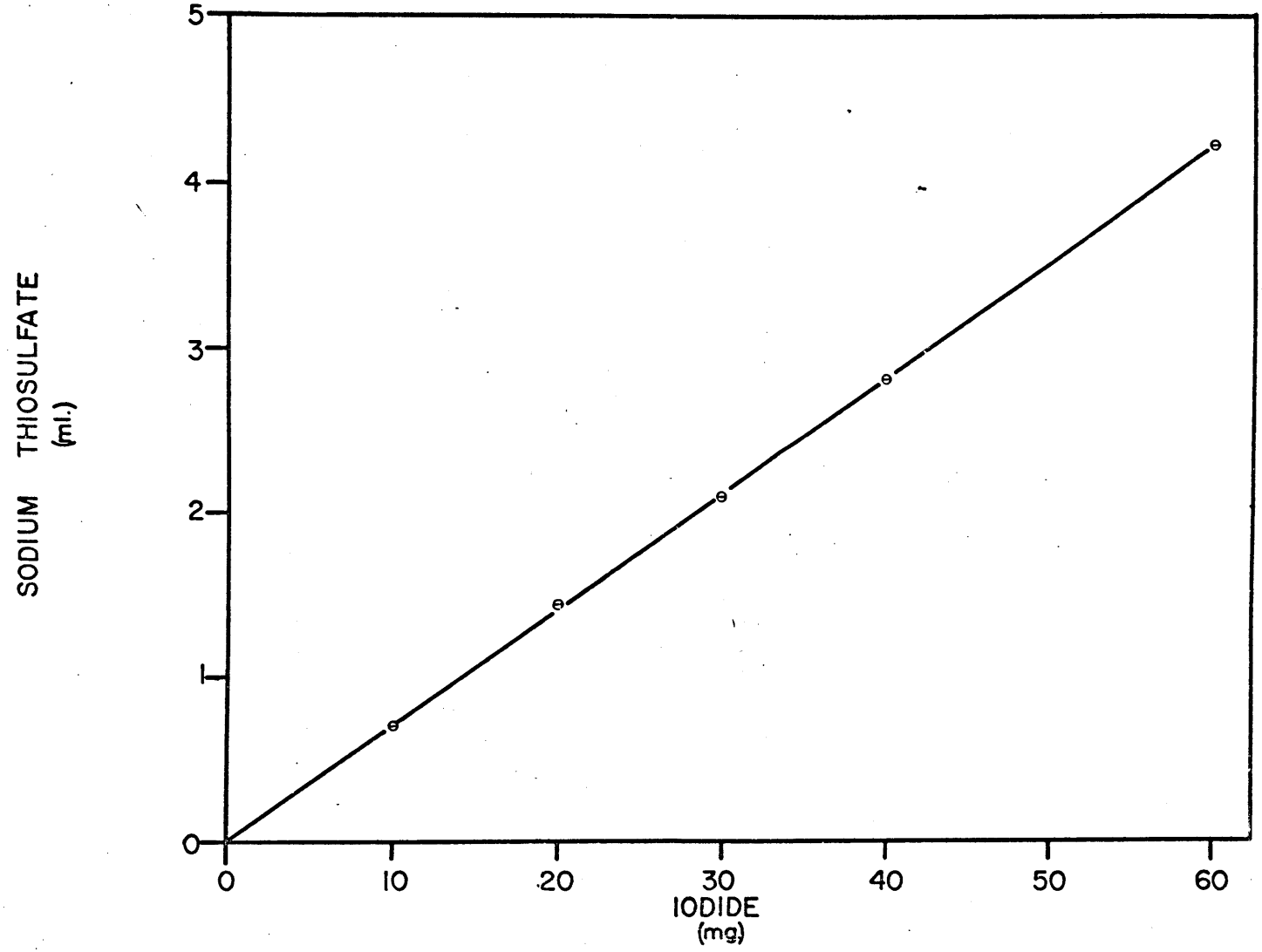

Figure 23 Calibration curve for iodide titration using sodium thiosulfate

After cooling, enough indicator was added to just barely color the solution. Ammonia was then added until the indicator turned blue, 3 ml of pH 10 ammonia-ammonium chloride buffer solution and 10 ml ethanol were then added to the beaker. Excess DCyTA was titrated with .1M magnesium chloride till the endpoint, .02M EDTA [(ethylenedinitrite) tetraacetic acid] was added dropwise until the blue coloration was again achieved. Ethanol was again added until about 40% of the solution was alcohol, approximately .02M $BaCL_2$ solution was added dropwise until a stable purple endpoint was reached.

A calibration curve, Figure 24, was made using a standard sulfate solution (4 mg/ml).

$$\text{Sulfate (mg)} = 1.869(\text{ml}) + 0.032 \qquad (44)$$

The predicted error is 1%.

In both analytical techniques, analyses were performed twice for each effluent volume.

B.4 Selective Ion Electrodes

Direct potentiometric measurements of sodium ion activity over 4 decades of concentration were made with glass electrodes (Beckman SelectIon Electrodes) that are highly specific to the sodium ion.

Measurements were made on the millivolt scale at the Beckman Zeromatic pH meter. The scale was expanded as outlined by Keegan and Matsuyama (47) using a decade

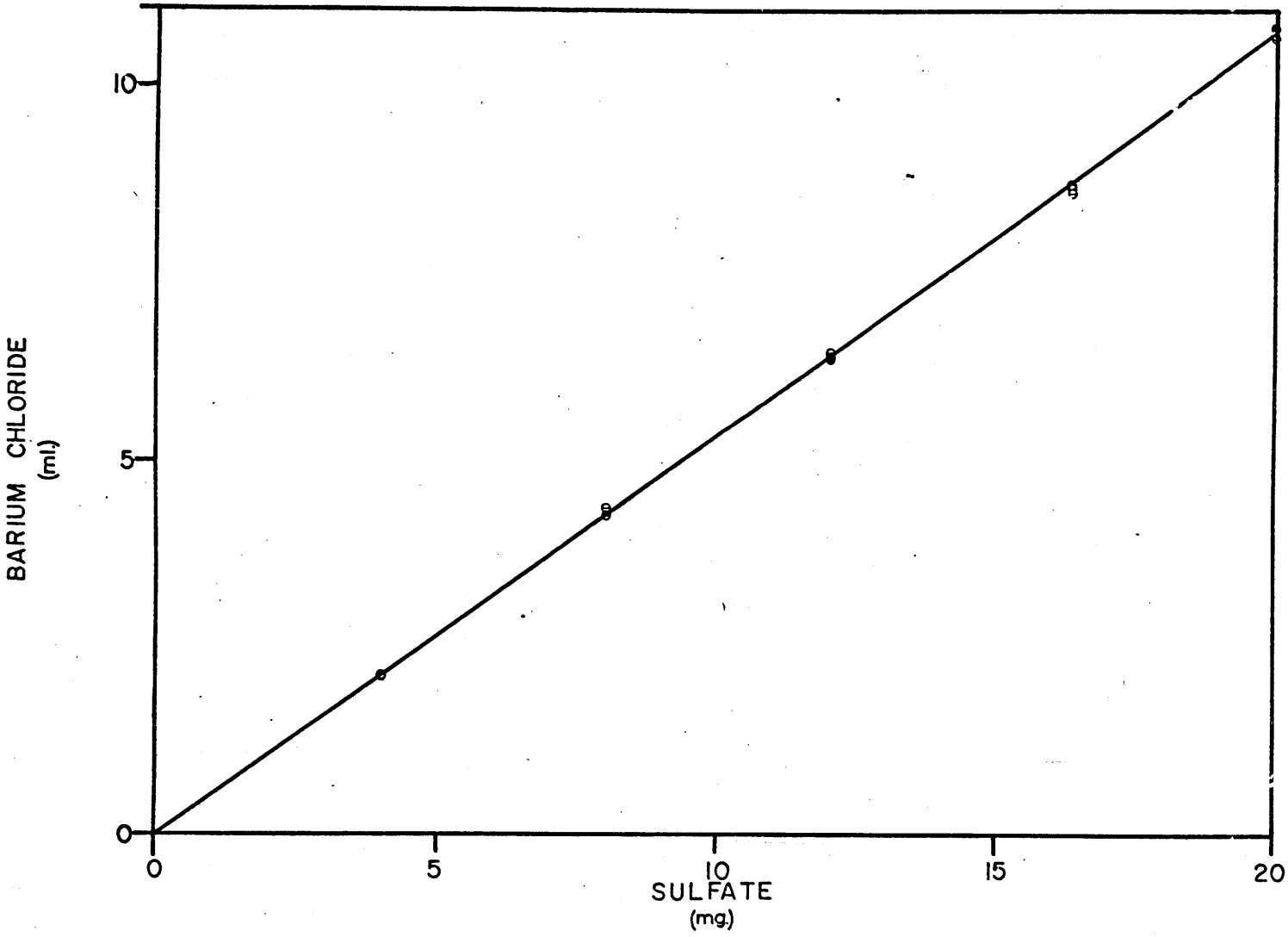

Figure 24 Calibration curve for sulfate titration using barium chloride

resistor box so that concentrations in the range $10.^{-2}$ - 1M and $10.^{-4}$ - 1M could be made. The asymetry control positioned the reading for 1M Na^{+} on scale reading 1.

Calibration curves, Figures 25 and 26, were made using 1M and .1M sodium chloride solutions. Other concentrations were made by dilution.

The pH of the sample solutions was adjusted between 8 and 9.

Error in the analysis was about 2.5%.

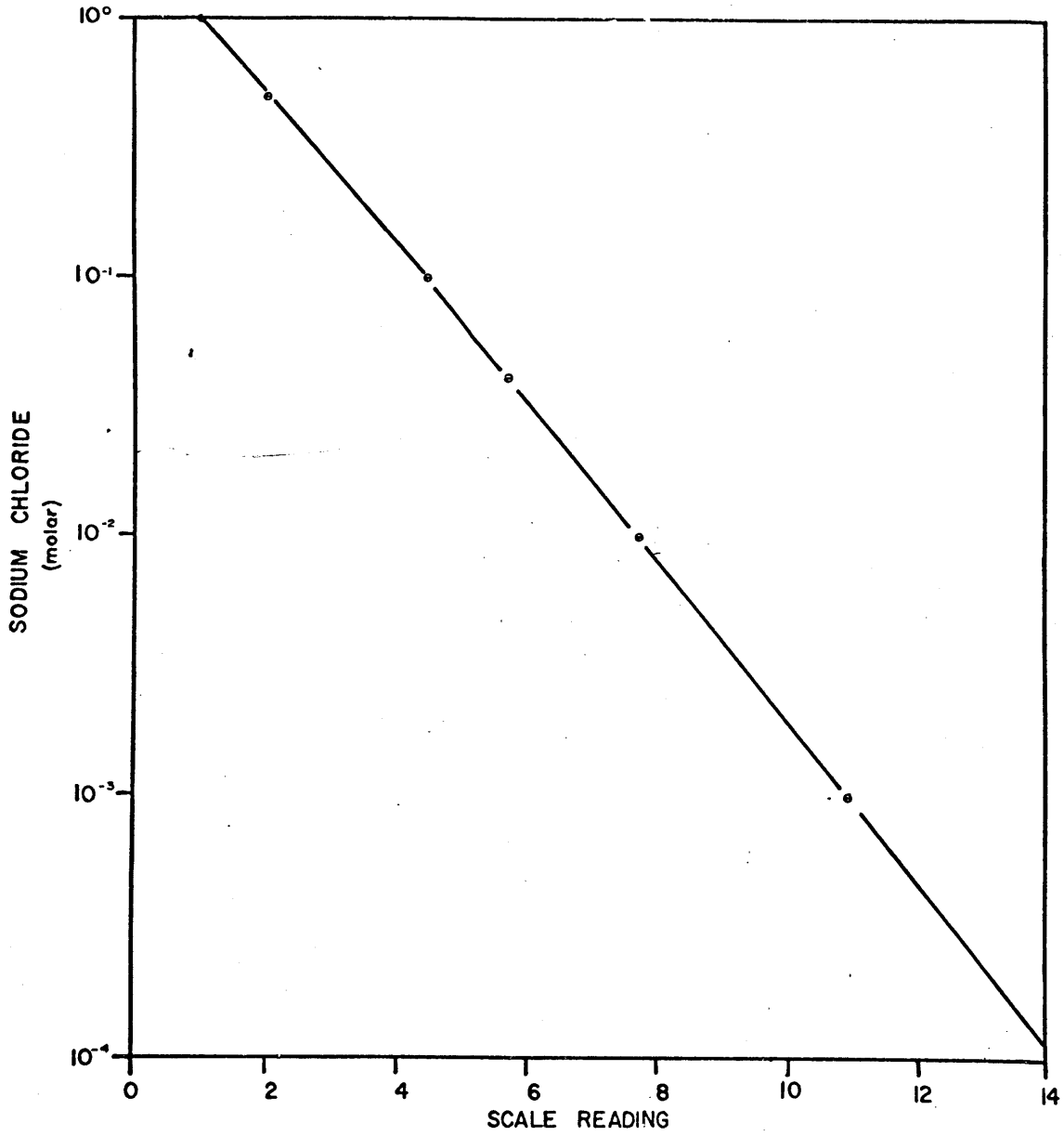

Figure 25 Sodium chloride calibration curve using Selection electrodes

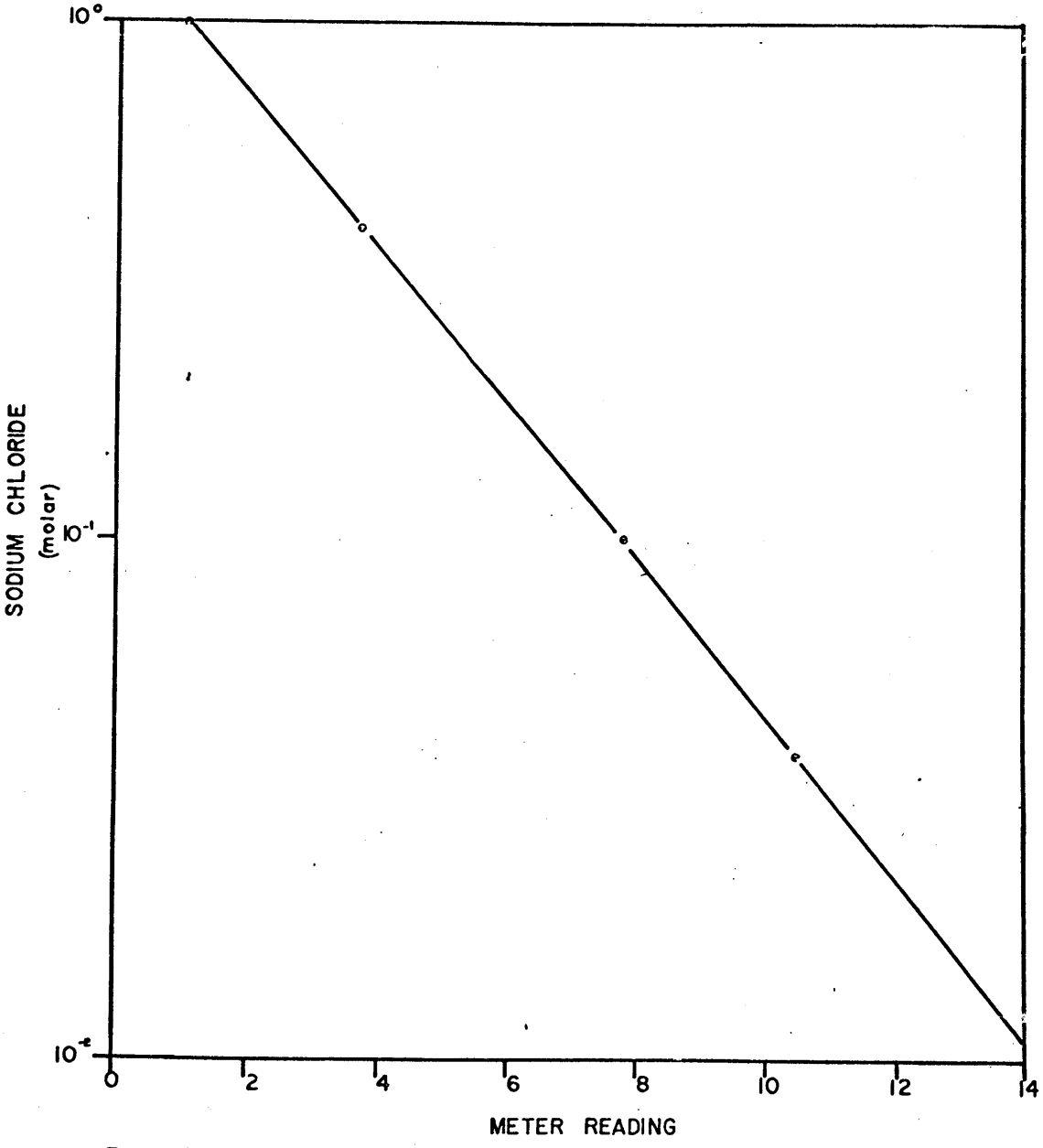

Figure 26 Expanded sodium chloride calibration curve using Selection electrodes

APPENDIX C

REFERENCES

1. D. Graves, Proceedings: Transactions of Power Reactor Systems and Components, Conference Williamsburg, Va., September 1-3, 1970.

2. J. Noble, Private Communication, Stone & Webster Engineering Corporation, 1970.

3. J. Marinsky, Ion Exchange, Vol. 2, Marcel Dekker, Inc., N.Y. (1966).

4. J. Inczedy, Analytical Applications of Ion Exchangers, Pergamon Press, Oxford (1966).

5. F. Helfferich, Ion Exchange, McGraw-Hill Book Company, N.Y. (1962).

6. J. Marinsky, Ion Exchange, Vol. 1, Marcel Dekker, Inc., N.Y. (1966).

7. D. Whitney and R. Diamond, Inorg. Chem., 2, 1284 (1963).

8. B. Chu, D. Whitney, and R. Diamond, J. Inorg. Nucl. Chem., 24, 1405 (1962).

9. F. Helfferich, Ob. cit. pp 134-6; 157-8.

10. F. Helfferich, Ibid. p. 283.

11. F. Nelson, J. Polymer Sci., 40, 563 (1959).

12. L. Siller, ed., Stability Constants of Metal-Ion Complexes, The Chemical Society, London, Sp Pub #17 (1964).

13. J. Kay, J. Bregman, A. Frad Kin, and J. D'Amico, Industrial and Engineering Chemistry 46 (5), 862 (1959).

14. Ion Exchange, Nalco Chemical Co., T.D. Index 120.01.

15. Ion Exchange, Nalco Chemical Co., T.D. Index 230.02.

16. V.V. Rachinskii, Russian J. Phys. Chem., 36(9), 1083 (1962).

17. K. Kraus and F. Nelson, Proc Intern. Conf Peaceful Uses At Energy, 1st Geneva 7, 113 (1956).

18. F. Nelson, T. Murase, K. Kraus, J. Chromatog, 13, 503 (1964).

19. K. Kraus and F. Nelson, The Structure of Electrolytic Solutions (W.J. Hamer, ed.), Wiley, New York, 1959, p 340.

20. T. Kressman and J. Kitchener, J. Chem. Soc., 1201 (1949).

21. J. Inczedy, Ob.cit., p 68.

22. F. Helfferich, Ob. cit., p 261, Eq. 6-12.

23. R. Kunin, Ion Exchange Resins, J. Wiley and Sons Inc., New York (1958).

24. J. Perry, ed., Chemical Engineers' Handbook, McGraw-Hill, New York (1963).

25. J. Friend, A Textbook of Inorganic Chemistry Vol. IX part II "Iron and Its Compounds" Charles Griffin and Co., London (1925).

26. J. Mellor, A Comprehensive Treatise on Inorganic and Theoretical Chemistry, Vol. XIV Fe(Part III), Co., Longmans, Green, and Co., London (1942).

27. K. Kraus and F. Nelson, ASTM Spec Tech Publ 195, 27 (1958).

28. F. Helfferich, Ob. Cit., p 166.

29. J. Carroll, "Absorption of Thorium on an Anion Exchange Resin," HW-70536 (1961).

30. J. Carroll, "A Mathematical Model for Ion Exchange Equilibrium," HW-72362 (1961).

31. Anolhin, V., Russian J. Phys. Chem. 38(8), 1100 (1969).

32. V. Rachinskii and S. Rustamov, Russian J. Phys. Chem. 38(3), 348 (1964).

33. V. Rachinskii and S. Rustamov, Russian J. Phys. Chem. 38(4), 480 (1964).

34. V. Rachinskii, K. Saldadze, and S. Rustamov, Russian J. Phys Chem., 40(3), 321 (1966).

35. I. Wilson, J. Am Chem Soc., 62, 1583 (1940).

36. V. Rachinskii and S. Rustamov, Russian J. Phys. Chem. 40(8), 970 (1966).

37. J.H. Noble, Patent 3,340,200, September 5, 1967.

38. F. Helfferich, Ob. Cit., pp 471-9.

39. R. O'Mara, Private Communications, Stone and Webster Engineering Corporation, 1971.

40. A. Calder, Photometric Methods of Analysis American Elsevier Publishing Co., New York (1969).

41. M. Griffing and M. Mellon, Anal. Chem, 19 (12) 1014 (1947).

42. F. Snell, C. Snell and C. Snell, Colorimetric Methods of Analysis, Van Nostrand Co., Princeton (1959).

43. S. Sauvin, Talanta, 8, 673 (1961).

44. D. Corvell, "Determination of Gamma-Ray Abundance Directly From the Total Absorption Peak," USNRDL-TR-288 (1958).

45. F. Treadwell, Analytical Chemistry, Vol II, Wiley, New York (1942).

46. L. Szekeres, Microchemical Journal, 13, 349 (1968).

47. J. Keegan and G. Matsuyama, Analytical Chemistry, 33, 1292 (1961).